https://doi.org/10.1016/j.ccr.2017.06.024

Functionalized 2D nanomaterials for gene delivery applications

Feng Yin[a,1], Bobo Gu[b,1], Yining Lin[c,1,*], Nishtha Panwar[b], Swee Chuan Tjin[b], Junle Qu[c], Shu Ping Lau[d], and Ken-Tye Yong[b,*]

[a]School of Chemical Biology and Biotechnology, Peking University Shenzhen Graduate School, Shenzhen 518055, China

[b]School of Electrical and Electronic Engineering, Nanyang Technological University, Singapore 639798, Singapore

[c]Key Laboratory of Optoelectronic Devices and Systems of Ministry of Education and Guangdong Province, College of Optoelectronic Engineering, Shenzhen University, Shenzhen, 518060, China

[d]Department of Applied Physics, The Hong Kong Polytechnic University, Hung Hom, Kowloon, Hong Kong

[1]These authors contributed equally to this work.

*Corresponding authors: linela10@yahoo.com (Yining Lin); ktyong@ntu.edu.sg (Ken-Tye Yong).

Contents

Abstract

During the last decade, two-dimensional (2D) nanomaterials have attracted tremendous interest in many different fields, including electrochemistry, energy storage/conversion, tissue engineering and biomedicine, owing to their unique chemical and optical properties. Recently, the promising potential of 2D nanomaterials，such as carbon based 2D nanomaterials and graphene analogues (such as transition metal dichalcogenides) as gene delivery systems has been explored and applied in various cancer theranostics. In this review, we focus on the applications of the functional 2D nanomaterials for gene delivery and optical imaging in cancer therapy. The properties and structure of different configurations of 2D nanomaterials are first summarized and compared. Then, the biomedical applications of functionalized 2D nanomaterials, particularly the potential of 2D nanomaterials as multifunctional delivery platforms and optical probes in gene delivery applications are briefly discussed and presented with a view to encourage clinical translations of this research.

Abbreviations

2D, two-dimensional; SCID, Severe Combined Immunodeficiency; CTL, cytotoxic T

cell lymphocyte; MHC, major histocompatibilty complex; TCR, T cell receptor; JAM1, junctional adhesion molecule 1; HIV-1, human immunodeficiency virus type 1; VSV-G, vesicular stomatitis virus G glycoprotein; LTR, long terminal repeat; CMV, cytomegalovirus; LDHs, layered double hydroxides; TMDs, transition mental dichalcogenides; TMOs, transition metal oxides; BP, black phosphorus; GO, Graphene oxide; CVD, chemical vapor deposition; CMOS, complementary metal–oxide–semiconductor; GIC, graphite intercalation compounds; PEI polyethylenimine; PAMAM, polyamidoamine; PS–NH_2, amine terminated polystyrene; PS, polystyrene; PLL, Poly-L-lysine; PAA, Polyacrylic acid; PVA, Poly(vinyl alcohol); PEG, Polyethylene glycol; MSNs, Mesoporous silica nanoparticles; QDs, Quantum dots; USGO, ultra-small GO; CS, Chitosan; CTAB, Cetyltrimethylammonium bromide; FA, folic acid; IONPs, iron oxide nanoparticles; pSiNPs, mesoporous silicon nanoparticles; Mo, molybdenum; W, tungsten; Nb, niobium, Re, rhenium; Ti, titanium; S, sulfur; Se, selenium; Te, tellurium; PVP, polyvinylpyrrolidone; PTT, photothermal therapy; LDHs, Layered double hydroxides; GRAS, Generally Recognized as Safe; HDTMA, hexadecyltrimethylammonium; RHEED, reflection high-energy electron diffraction; MBE, molecular beam epitaxy; PLD, pulsed laser deposition; ALD, atomic layer deposition; PDT, photodynamic therapy; NIR, near-infrared; BPQDs, BP quantum dots; PLGA, poly(lactic-co-glycolic acid; ROS, singlet oxygen species; UCNPs, upconversion nanoparticles; siRNA, small interfering RNA; GSH, glutathione.

Key words：2D nanomaterials; gene delivery; imaging; graphene; cancer

1. Introduction

The fast pace development of present-day technology and high degree of industrialization offer better living conditions to people on one hand but serious environmental pollution and enormous daily pressure on the other. As a result of this stress, many diseases get induced and become the critical risk factors of death. According to the global diseases statistics in 2016, cardiovascular disease is the leading cause of death, which is estimated to account for more than 17.3 million deaths in a year [1]. Cancer, which has existed for over a thousand years has now become the second most devastating disease with limited effective treatments. Moreover, other diseases, such as diabetes, pulmonary tuberculosis, hepatic failure and neurology have also become threats to human health (Figure 1A) [2]. With the

growing worldwide incidence and mortality rates of different diseases, the demand for clinical biomedicine is growing sharply.

Due to the numerous triggers of different diseases, various kinds of therapies have been developed with certain therapeutic efficiency. For example, surgery and chemoradiotherapy are the commonly used methods for cancer treatment; chemotherapy is the main method for cardiovascular disease and pulmonary tuberculosis. In the last decade, gene therapy has gathered tremendous research interest and is considered as the promising candidate for treating diseases with extraordinary development. Gene therapy is a novel approach with goals of repairing or replacing the direct cause of genetic diseases by inserting nucleic acid polymers into patient cells, and is expected to be an effective strategy for the treatment of cancer, cardiovascular disease, viral infections and other genetic diseases (Figure 1B) [3, 4]. The recombinant DNA technology, discovered in the 1970s, served as a fantastic tool for gene regulation. In 1990, SA Rosenberg and co-workers first attempted to introduce foreign genes into human cells by retroviral-mediated gene transduction [5]. It was the first such successful attempt which was later approved for nuclear gene transfer study in humans and paved the way for a new era in biomedicine. In the following decades, scientists devoted great efforts to identify mutations involved in human diseases and utilized the therapeutic genes for disease treatment. The first clinical success of X-linked Severe Combined Immunodeficiency (SCID) by gene therapy in 2006 [6] led to gene therapy studies for retinal diseases [7], ADA-SCID [8], lymphocytic leukemia [9], Parkinson's disease [10] and cancer [11],

and achieved some preliminary effects. However, due to the poor stability, low-efficient transfection into cells and toxicity of nucleic acid drugs, gene therapy is still an experimental technique and is currently in preclinical research stage. Effective gene therapy depends on the efficient transfection and stable expression of foreign genes in the target cells and tissues, which is closely related to the delivery systems. Therefore, development of efficient gene delivery systems is a major issue for further applications of gene therapy in biomedical field. The gene therapy delivery systems, in the present form, can be divided into two categories: viral vectors and non-viral vectors (Figure 1C) [12, 13].

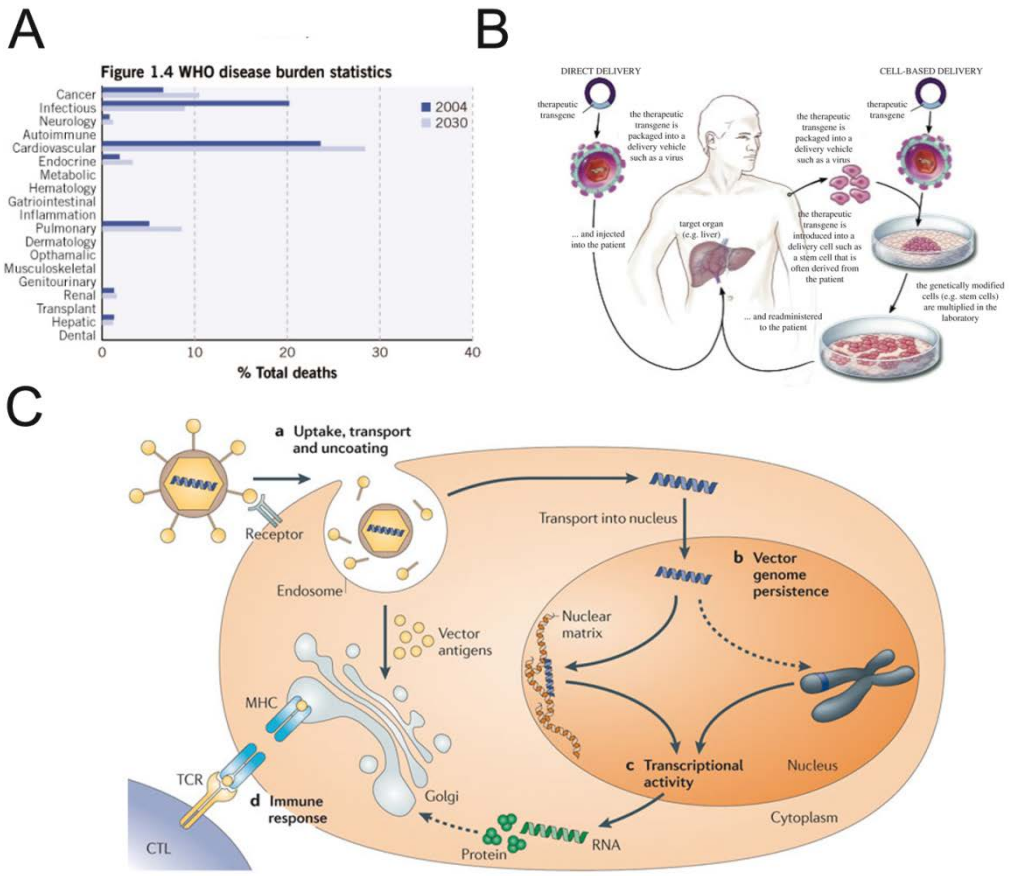

Figure 1 Disease statistics and gene therapy. **(A)** WHO disease burden statistics for the top causes of mortality and morbidity worldwide between 2004 and 2030. (Reproduced from Ref. [2] with permission of Nature Publishing Group) **(B)** Strategies for delivering therapeutic transgenes into patients. (Reproduced from

Ref.[3] with permission of Royal Society) **(C)** The processes of successful gene therapy in cells. **a.** Gene vectors bind to the cell membrane and are internalized by various processes. **b.** It undergoes further processing upon reaching the nucleus. Depending on the vector, the DNA can exist as an episomal molecule (and associate with the nuclear matrix) or it can be integrated (by covalent attachment) into the host chromosome. **c.** Transcriptional activity. **d.** The immune response can limit the viability of the transduced cells and/or the expression of the transgene product. (Reproduced from Ref.[4]with permission of Nature Publishing Group)

2. Viral vectors

In order to deliver nucleic acid drugs sufficiently and safely into the host cells, the virus vectors for gene therapy should have the following basic characterizations: (1) ability to package and carry exogenous genes with them; (2) transfer the foreign genes to the targets with high expression; (3) possess no pathogenicity for host cells. However, most wild-type of viruses are pathogenic to the organisms. Therefore, it is necessary to transform viruses to be suitable for using in human bodies [14]. Due to the diversity of viruses and complicated interdependent relationship between viruses and host cells, the life cycle and molecular mechanism of viruses are still unclear which limit further applications of viruses as gene delivery systems in clinical biomedicine. In the last 2 decades, just a few types of viruses have been successfully transformed and applied for gene delivery, including retroviruses [15], adenovirus [16] and herpes virus (such as simple herpes virus [17], vaccinia virus [18] and Epstein-Barr virus [19]). Adenovirus is an efficient vehicle for gene delivery, particularly in the treatment of cancer and cardiovascular diseases. However, the innate cytotoxicity and non-selectivity of adenovirus impedes further clinical applications [20]. Mercier et al. developed a novel kind of chimeric adenovirus vectors, which could specifically target cells expressing junctional adhesion molecule

1(JAM1) and had low immunogenicity [21]. For the non-dividing cells such as hepatocytes, myoblasts, neurons and hematopoietic stem cells, lentivirus has been considered as the proper gene delivery system. Verma and co-workers constructed a new series of lentivirus vectors based on human immunodeficiency virus type 1 (HIV-1) which were pseudotyped with the vesicular stomatitis virus G glycoprotein (VSV-G) as well as replaced the long terminal repeat (LTR) region with the cytomegalovirus (CMV) promoter. These lentivirus vectors could stably integrate into the host cell genome and obtained long-term expression of transgenes, without cellular immune response [22]. However, this technique imposes some major concerns that restrict their clinical translation [23, 24]: (1) random integration of virus into the host genome induces gene mutation and activation of oncogenes; (2) the insertion capacity of virus is limited (8kb); (3) the preparation of transformed viruses is complicated and costly; (4) the uncontrollable virus titer affects transfection efficiency and cell death; (5) the instability of virus in the physiological environment. Although the artificially transformed virus vectors have low immunogenicity and transfection efficiency, these problems should be solved before translating for clinical research.

3. Non-viral vectors

Non-viral vectors are a strong alternative for gene and drug delivery as they possess low pathogenicity, facile preparation, reusability and biosafety [12, 25-27]. Compared to these viral vectors, biosafety is the major advantage of non-viral vectors, such as liposomes [27-29], peptides [30, 31] and inorganic nanomaterials [32, 33], which

attracts significant attention in gene/drug delivery for biomedicine. In 1990s, cationic liposomes, composed of positively charged hydrophilic head and hydrophobic tail, were the most widely used non-viral vectors for gene therapy [34]. Based on electrostatic interactions, the positively charged group could bind with nucleic acid drugs to form uniquely compacted structures called lipoplexes. Inspite of the positive charge of lipoplexes that could facilitate cellular uptake of nucleic acid drugs without cytotoxicity, the short half-time and rapid removal from the body circulation impeded the *in vivo* applications of liposomes. Although polyethylene glycol is applied as a surface shielding to enhance the half-time of lipoplexes, the transfection activity is reduced by more than 85% in melanoma cells [30]. In 1997, Legendre et al. fabricated a peptide-based gene delivery system that resulted from the conjugation of dioleoylphosphatidylethanolamine-N-[3-(2-pyridyldithio)propionate] with melittin [35]. This work represents a novel peptide-based gene delivery system with low cytotoxicity and high biocompatibility. However, the instability, antigenicity and limited loading capacity of peptides are the fatal weaknesses for further clinical applications. Self-assembly peptide nanoparticles have demonstrated promising performance in gene delivery applications recently [36].

In the last decade, inorganic nanomaterials have drawn increasing attention and are utilized as gene/drug delivery systems [32, 37] and optical probes [38] in biomedicine. Gold nanoparticles [39, 40], mesoporous silica nanoparticles (MSNs) [41, 42], magnetic nanoparticles [43, 44] and quantum dots (QDs) [45, 46] represent inorganic nanomaterials that play important roles in developing gene delivery and optical

imaging. Ever since its first discovery by Geim et al. in 2004 [47], graphene research has exponential risen and it has become one of the hottest nanomaterials during the next ten years. The unique optical properties, higher specific surface areas, thinner sheet structures and superior biocompatibility make graphene suitable for gene delivery in comparison with other nanomaterials, which pave a new era for the applications of 2D nanomaterials in biomedical field [48, 49].

2D nanomaterials are a newly emerging field, which have ultrathin structure with a high degree of anisotropy and chemical functionality [50, 51]. Compared to other conventional nanomaterials, 2D nanomaterials possess extraordinary mechanical, chemical and optical properties, and are suitable for a wide range of applications, including electronics [52], catalysis [53], energy production and storage [54], biosensor [55] and biomedicine [48, 56]. For applications in biomedicine, especially gene delivery and optical imaging, 2D nanomaterials have promising potential and are considered as the appropriate gene delivery systems due to their distinct merits: (1), They possess the highest specific surface areas among the various kinds of nanomaterials to adsorb any amount of nucleic acid molecules; (2) regardless of low or high concentrations, the biomedical nanocomposites with well-defined mechanical properties can be composed by 2D nanomaterials, because of their exceptional surface-to-volume ratios and typical physicochemical properties; (3) 2D nanomaterials have the thinnest structures, which are sensitive to the external lights and can be utilized in optical imaging and photothermal therapies [12, 56]. Recently, a series of 2D nanomaterials have been developed as drug delivery systems for

biomedicine, such as graphene [57], silicate clays [58], layered double hydroxides (LDHs) [59], transition mental dichalcogenides (TMDs) [60] and transition metal oxides (TMOs) [61, 62]. In the next few sections, we focus on the current advances of graphene, silicate clays, layered double hydroxides (LDHs), transition mental dichalcogenides (TMDs) and transition metal oxides (TMOs) as gene delivery systems for disease theranostics（Figure 2）. The structural properties and biomedical applications of these diverse 2D nanomaterials are summarized respectively. Furthermore, a novel kind of 2D nanomaterial, black phosphorus (BP) is discussed in this content, which has been considered as a fancy 2D nanomaterial with unexpected potential in biomedicine.

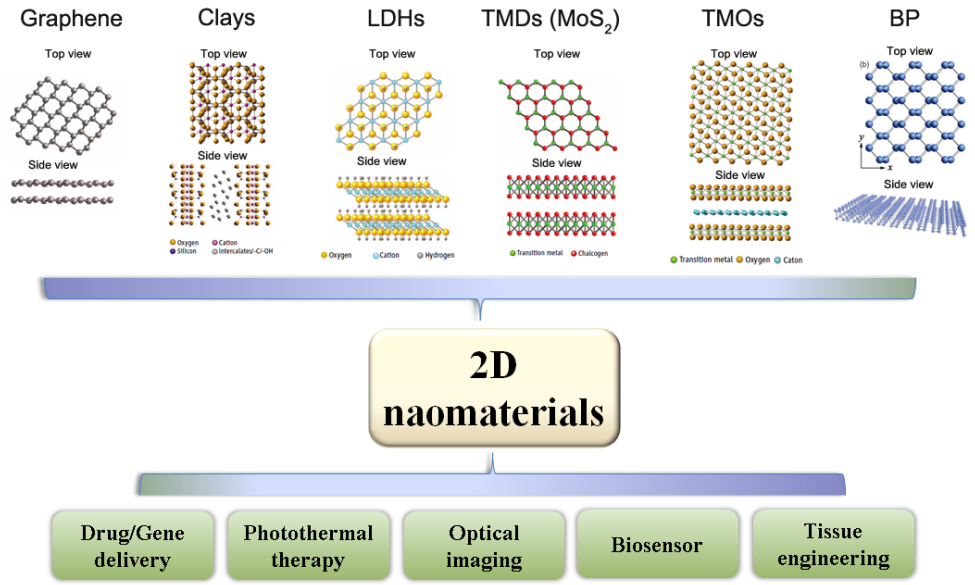

Figure 2 The structures and biomedical applications of six representatives of 2D nanomaterials: graphene, silicate clays, LDHs, TMDs, TMOs and BP. Reproduced from Ref.[62-64] with permission of American Association for the Advancement of Science, American Physical Society and 2016 WILEY‐VCH Verlag GmbH & Co. KGaA, Weinheim)

3.1 Graphene and Graphene oxide (GO)

In 2004, Novoselov and co-workers successfully separated 2D graphene from

graphite [47], which was the first discovery of graphene and marked the beginning of a new era in nanotechnology. In the past years, Graphene has been considered as the "new wonder nanomaterial" and has inspired a wave of research on 2D nanomaterials. This novel nanomaterial is a single layer of carbon atoms in the form of graphite, with a hexagonal ring layered structure, making it the thinnest nanomaterial with a single carbon atom thickness [65]. Owing to the unique physical and chemical properties, graphene is widely applied in many different fields, including electrode materials, ultracapacitors, solar cells, sensors and energy storage.

In recent years, the multi-functional graphene has attracted great attention and demonstrated to have excellent advantages for biomedical applications: (1) The strong absorption in the near infrared region induces photon-electron interactions in order to generate heat, which are widely used as the photothermal reagents for tumor and other diseases treatments *in vivo*; (2) Based on the special optical and high biocompatible properties, graphene is an excellent contrast agent without toxicity for biological imaging, including fluorescent imaging, magnetic resonance imaging (upon loading with magnetic agents like Fe_3O_4) and photoacoustic imaging; (3) The large specific surface area and the exceptional surface-to-volume ratio are the unparalled advantages of graphene to be used in drug or gene delivery systems in biomedicine; (4) In addition, although bare graphene nanomaterials show some toxicity in *in vivo* experiments, the facile surface-functionalization of graphene greatly enhances the biocompatibility and reduces the toxicity.

3.1.1 The preparation of graphene 2D nanomaterials

During the past decade, scientists have devoted great efforts to study graphene and developed several methods to fabricate graphene for different applications. The first attempt for the preparation of graphene was made by Fernandez, an electron microscopist, who produced graphene through micromechanical exfoliation from graphite to obtain an improved microscopically supporting membrane [66]. These millimeter sized graphene sheets were then observed to be as thin as 5 nm by electron microscopy [67]. At present, there are four major methods for the preparation of graphene materials (Figure 3), including mechanical cleavage [68], epitaxial growth [69], chemical vapor deposition (CVD) [70] and chemical method [71].

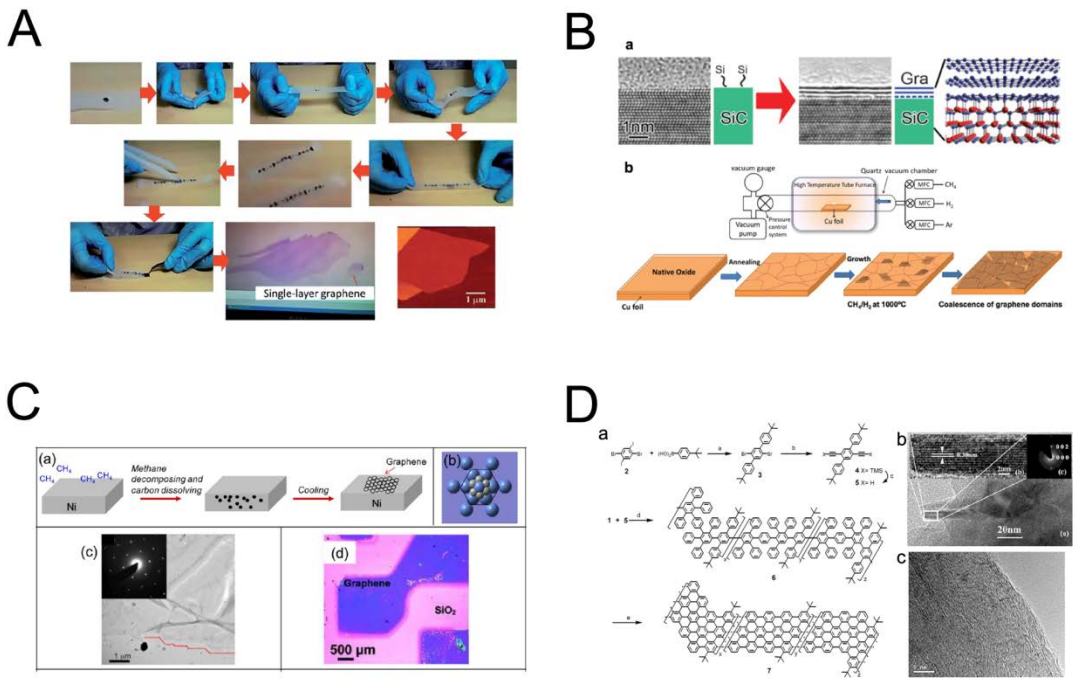

Figure 3 The four major methods for the preparation of graphene. (A) A stepwise illustration of the Scotch-tape based micromechanical cleavage of HOPG. Reproduced from Ref. [72] with permission of Royal Society of Chemistry. (B) The schematic for epitaxial synthesis and CVD of graphene. Reproduced from Ref. [73] with permission of Royal Society of Chemistry. (C) The schematic diagram of CVD of graphene and TEM image of graphene edges. Reproduced from Ref. [70] with permission of American Chemical Society. (D) The synthetic process of graphene by

chemical method and TEM images of the graphite ribbon. Reproduced from Ref. [74] with permission of American Chemical Society.

By chemical oxidation, different kinds of oxygenated functionalities (such as carboxyl, hydroxyl and epoxy) are introduced into graphite structure to form GO [75]. These oxygenated functionalities expand the layer separation and enable the material to disperse in organic solvents, water and different matrixes easily. Moreover, the properties of GO can be adjusted manually by chemical modifications with these oxygenated functionalities for greater adaptability for desired applications. In 1859, GO was first fabricated from graphitic powder with potassium chlorate in concentrated fuming nitric acid [76]. However, this method is complicated and unsafe with low yield. Hummers and Offeman developed a less hazardous and more efficient method for the synthesis of GO using a mixture of sodium nitrate, potassium permanganate, and concentrated sulfuric acid [77]. This method is the easiest and widely used approach way to get a large sum of GO and graphitic derivatives. In this method, natural graphite is reacted with strong acids and strong oxidizing reagents to form GO, which possesses a certain amount of epoxy, hydroxyl or carboxyl groups on the surface for functionalization to target molecules such as peptides or antibodies.

3.1.2 Multi-functionalization on the surface of GO

Although GO has good stability in aqueous solution, the physiological solutions such as PBS, saline or cell culture medium cause the re-aggregation of GO, probably because of the charge screening effect generated by the presence of salt ions [78]. Therefore, scientists have explored numerous kinds of methods to modify the surface of GO to improve its stability for *in vitro* and *in vivo* biomedical applications [79, 80].

To date, various methods for GO surface modification have been reported, including covalent and noncovalent modifications. In addition, a lot of inorganic nanoparticles have been utilized to modify the surface of GO, thereby obtaining the functional GO complexes. The different surface modifications of GO with diverse biomedical applications are listed in Table 1.

Table 1. Examples of molecules/particles conjugated on the surface of GO.

Modification type	**Molecules/Particles name**	**Reference**
Noncovalent interaction	DNA	[81, 82]
	protein	[83]
	peptide	[84, 85]
	polyethylenimine (PEI)	[86, 87]
	polyamidoamine (PAMAM)	[88]
	amine terminated polystyrene (PS–NH_2)	[89]
	Phospholipid	[90]
	chitosan-ionic liquid conjugation	[91]
	chitosan/dextran	[92]
Covalent interaction	Linear polystyrene (PS)	[93]
	Poly-L-lysine (PLL)	[94]
	Sulfonic acid	[95]
	Polyacrylic acid (PAA)	[96]
	Poly(vinyl alcohol)(PVA)	[97]
	Polyethylenimine(PEI)/ Polyethylene glycol(PEG)	[98]
	Chitosan	[99]
Nanoparticles decoration	Fe_3O_4 nanoparticles	[95]
	Gold nanoparticles	[82]
	Mesoporous silica nanoparticles (MSNs)	[100]
	Quantum dots(QDs)	[101]
	Titanium oxide nanoparticles	[102]

3.1.3 Multi-functional GO based gene delivery systems

Compared to chemotherapy, gene therapy requires more effective and stable delivery systems to function in the target cells and tissues. In the past decade, many

kinds of nanoparticles have been used as carriers for gene delivery to improve the therapeutic efficacy and reduce side effects. As the “new wonder nanomaterial”, GO-based nanocarriers play a significant role in gene therapy due to their distinct advantages such as large surface area, facile surface-functionalization and good biocompatibility. First, the amount of carboxyl groups on the surface of GO can react with various molecules for targeting and multi-functionalization. Secondly, the high specific surface area endows GO the ability to deliver drugs or nucleic acid molecules sufficiently and efficiently. Thirdly, the sustained release effect assists GO in enhancing the medication persistency. Moreover, GO-based nanosheets have the thinnest structures, which are sensitive to external lights and can thus be utilized in optical imaging and photothermal therapies. Briefly, GO with the plentiful carboxyl groups on the surface can be functionalized by non-covalent and covalent interactions with diverse polymers and molecules to achieve the efficient nucleic acid molecules delivery for biomedical applications.

(1) Covalent interaction

Although gene therapy possesses promising therapeutic potential for the genetic treatment of chronic diseases, the free nucleic acid molecules are fragile with fast degradation and have limited uptake efficiency because of the negative charge which restrict further applications of gene therapy *in vivo*. However, GO nanosheets carry negative charge because of the numerous carboxyl groups. To obtain the idea of GO-based gene delivery systems, various positive polymers are decorated on the surface of GO to change the surface charge and enhance its biocompatibility. For

instance, the positive polymer PEI is extensively bound to GO for gene delivery. Zhou et al. utilized PEI to covalently conjugate on the surface of ultra-small GO (USGO) by a carbodiimide cross-linking reaction between –COOH groups of USGO and –NH2 of PEI (Figure 4A) [103]. The PEI grafted USGO-based DNA delivery system could transfect plasmid DNA into mammalian cell lines and zebrafish embryos with up to 95% and 90% efficiency respectively, which exhibit better transfection efficiency as against commercial transfection reagents with lower toxicity (Figure 4B and 4C). Besides the covalent interaction between PEI and GO, PEI can also bound directly to GO by electrostatic interaction due to its positive charge. The GO-PEI complex is not only less cytotoxic, but is also rich in positive charge for successful loading of mRNA in cells to mediate generation of “footprint-free” iPSCs (Figure 4D and 4E) [104]. Another commonly used polymer is polyethylene glycol (PEG), which is considered as a non-toxic, non-immunogenic and hydrophilic reaction medium for functionalization of various nanomaterials [105]. Zhang and co-workers developed a dual-polymer-functionalized nanoscale GO with both PEG and PEI to transfect plasmid DNA into Drosophila S2 cells. This GO-PEG-PEI based gene delivery vector offers 7-fold and 2.5-folder higher efficiency compared with PEI and Lipofectamine-2000, which is even more distinct when transfecting cells with lower-quality linearized DNA [98]. Chitosan (CS), a naturally occurring linear cationic polysaccharide, is also widely applied for the modifications of nanomaterials, due to its good biocompatibility, biodegradability, low immunogenicity, and antibacterial property [106]. CS can be covalently bound on the surface of GO by a

facile amidation process, and can thus effectively encapsulate plasmid DNA to form compact complexes with a reasonable transfection efficiency and minimum cytotoxicity [99].

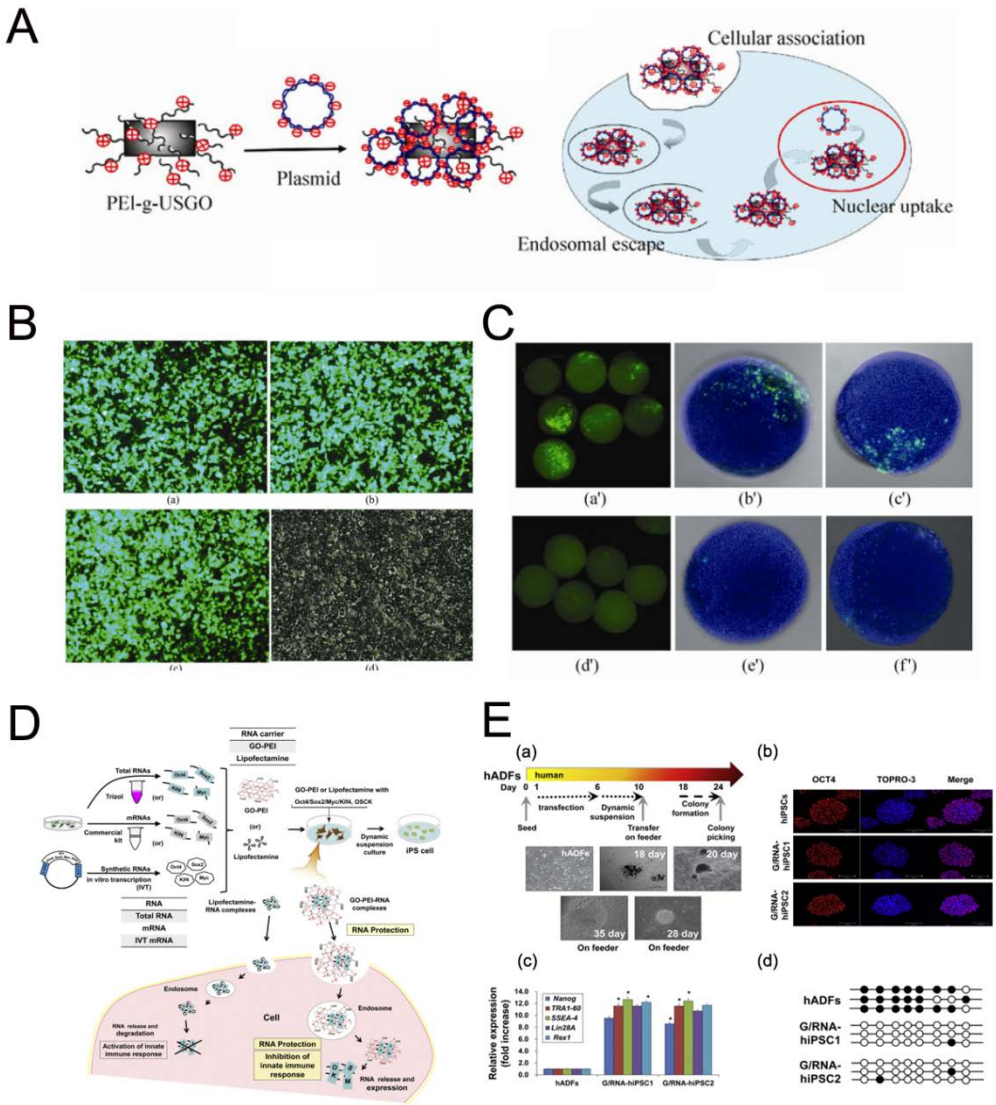

Figure 4 PEI modified GO as gene delivery systems for biomedical applications. (A) Schematic representation of plasmid condensation using PEI-USGO for gene transfection. (B) Fluorescence images of transfection of pEGFP using PEI-USGO in H293T cells at (a) 24 h, (b) 48 h, and (c) 72 h respectively. (C) Fluorescence images of pEGFP-transfection into zebrafish embryos using PEI-g-USGO (a'-c') or lipofectamine (d'-f') 6 h after injection, respectively. (Reproduced from Ref [103]. with permission of Tsinghua University Press and Springer-Verlag Berlin Heidelberg.) (D) A schematic diagram describing the generation of footprint-free iPSCs by GO-PEI complex-mediated mRNA delivery into cells. (E) GO-PEI-RNA complexes for RNA

delivery into somatic cells. (Reproduced from Ref.[104] with permission of Elsevier B.V.)

(2) Non-covalent interaction

In addition to the covalent interaction, GO can also be bound with polymers or biological macromolecules by hydrophobic force, π-π accumulation and electrostatic interaction. Cationic surfactants (such as Cetyltrimethylammonium bromide (CTAB) [107]) and hydrophilic macromolecules (such as aromatic organic molecules [108]) are functionalized non-covalently on the surface of GO to enhance its water solubility. Moreover, biocompatible polymers are applied for GO modifications to obtain higher biocompatibility and lower cytotoxicity for biomedical applications. Zhi et al. modified GO with PEI and PSS (sodium 4-styrenesulfonates) (PSS) through the layer-by-layer assembly method, which successfully co-delivered anti-cancer drugs and microRNA in breast cancer MCF7 cells. This GO-based co-delivery system showed superior transfection efficiency and enhanced the therapeutic efficacy in drug-resistant tumor cells [109]. In our studies, we constructed functionalized GO nanoparticles as a novel gene delivery system by conjugating folic acid (FA), NH_2-mPEG-NH_2 (5k) and Poly-allylamine hydrochloride (PAH) onto GO nanosheets for *in vivo* cancer targeting and small interfering (siRNA) delivery (Figure 5). With low-toxicity, biocompatibility high loading efficiency and photothermal properties, the multi-functionalized GO delivery system exhibits promising potential in targeted gene therapy and photothermal effect for pancreatic cancer treatment [110].

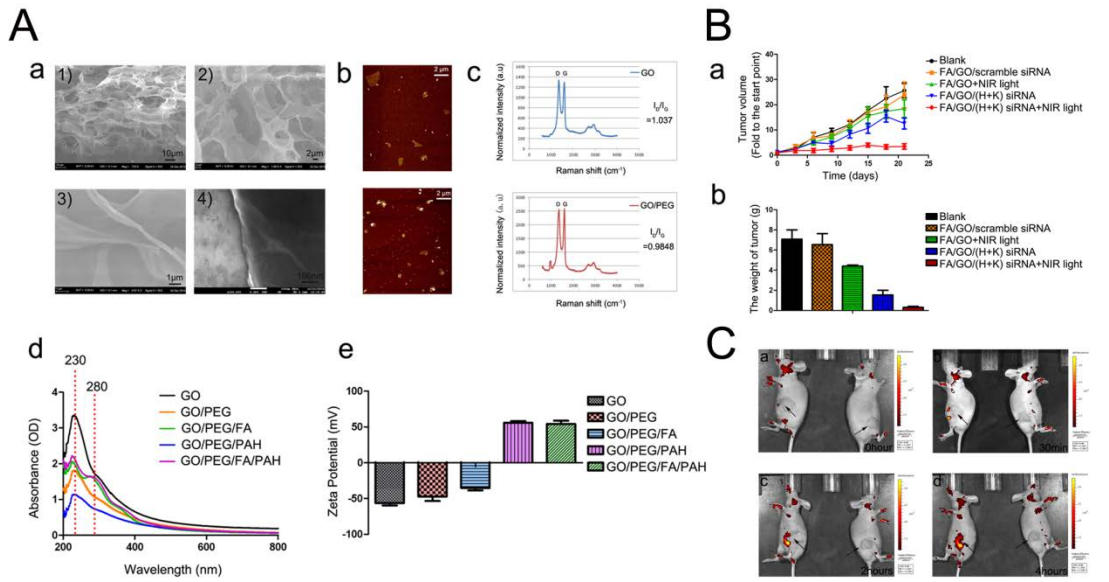

Figure 5 The FA/PEG/PAH modified graphene oxide (GO) for tumor inhibition and optical imaging *in vivo*. (A) Characterization of synthesized ORMOSIL nanoparticles; (a) Scanning electron microscope of the monolayer 2D GO nanosheets. (b) AFM images of GO before and after PEGylation. (c) Raman spectra of GO and PEGylated GO. (d) Absorption spectra of different GO-based nanocarriers. (e) Surface zeta potential of the different GO nanoformulations. Values are means ± SEM, n = 3. (B) *In vivo* tumor inhibition and luminescence imaging by different GO based nanocomplexes [110].

(3) Encapsulating nanoparticles in GO

To acquire improved stability and biocompatibility, GO is functionalized covalently or non-covalently with numerous polymers (such as PEG, PEI and PAH) and biomacromolecules. In addition, inorganic nanoparticles, including magnetic iron oxide nanoparticles (IONPs), silica nanoparticles and gold nanoparticles are encapsulated in GO to form novel GO nanocomplexes for biomedical applications. According to the protocol reported by Yang et al., biocompatible polymers, magnetic particles and element radiolabels can be functionalized on GO, which show multi-functionalization and high reproducibility for various applications in

biomedicine [111]. To obtain high yield, Xu and co-workers successfully encapsulated gold nanoparticles in GO through electrostatic self-assembly [111]. The GO-gold nanoparticles complexes were further linked with PEI to change the surface charge, which provided an abundance of positive charge for DNA delivery. This novel gene vector forms a class of novel nanovectors based on GO for gene therapy. Moreover, the biodegradable mesoporous silicon nanoparticles (pSiNPs) were coated by GO nanosheets as protective “shells” [112]. This pSiNPs-GO based nanocarrier shows a high level of siRNA loading, protects the siRNA from nucleolytic degradation and releases active siRNA slowly in a useful timescale.

To date, many related studies have confirmed that GO can be efficiently used as a gene transfection nanocarrier through appropriate surface modification as it possesses incomparable advantages including high loading efficiency, facile surface-functionalization and good biocompatibility. However, the metabolism and toxicity of GO *in vivo* are disconcerting and thus should be explored explicitly for further clinical applications.

3.2 Transition metal dichalcogenides (TMDs)

During the past few years, a newly emerging class of 2D-nanomaterials, transition metal dichalcogenides (referred to as TMDs), which are considered as one of the 2D graphene analogues, also attracted considerable attention due to their unique physical, chemical and electronic properties. The chemical formula of TMDs is MX_2, M denotes a transition metal element (e.g., molybdenum, tungsten, niobium, rhenium, titanium) and X refers to a chalcogen (such as sulfur, selenium and tellurium).

Typically, a single transition metal sulfide exhibits an X-M-X sandwich structure (Figure 6A). Although the Van der Wals forces between layers are very weak but strong covalent bonds exists in-plane. TMDs can be exfoliated into monolayer or multilayer nanosheets as graphene. In addition, 2D TMDs (e.g. ReS_2, $ReSe_2$) have weak interlayer coupling and a unique distorted 1T structure, which exhibit in-plane anisotropic properties (Figure 6B-D) [113]. Although TMDs have similar structures as graphene with planar topology and ultrathin thickness (single or several atomic layers), a direct band gap structure of TMDs improves the efficiency of optical emission and provides an opportunity for the preparation of high-performance optoelectronic devices in the far-infrared to visible light range. Therefore, the distinctive physicochemical or biological properties, composition and surface status enable TMDs to be ideal candidates of graphene-based nanomaterials for numerous applications including electronic devices [114], transistors [115], energy storage devices [116] and catalysis [117]. Due to the similarities in the morphology and properties between graphene and TMDs, the success of graphene has encouraged the exploration of TMDs for drug delivery [118], photothermal (PTT)/photodynamic therapy (PDT) [119], diagnostic imaging [119], and biosensing [120].

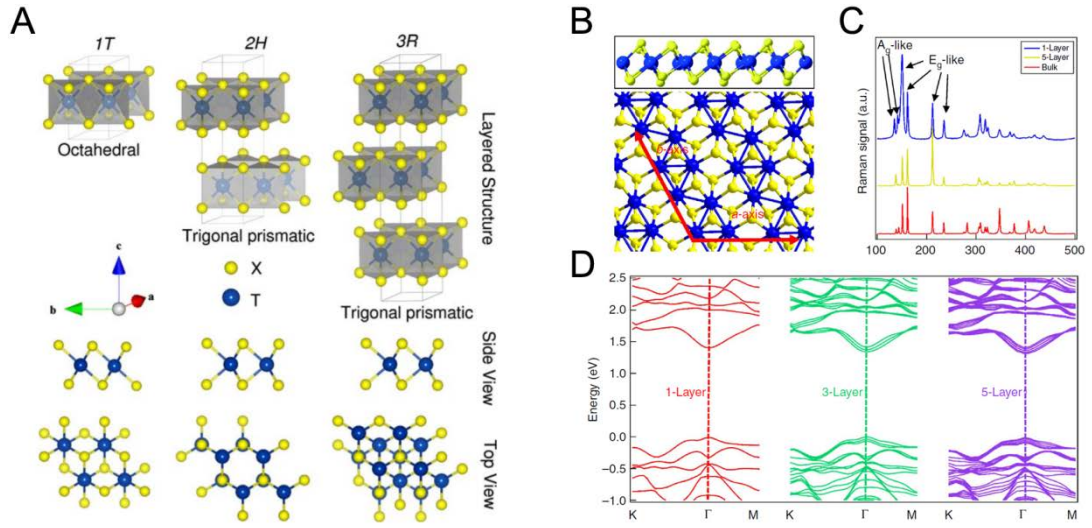

Figure 6 Characterization and band structure of thin-layer TMDs. (A) Structural representation of 1T, 2H and 3R TMC polytypes and their corresponding metal atoms coordination. (B) Crystal structure of monolayer ReS_2 with a side view in the top panel and a top view in the bottom panel. The directions of *a* and *b* axes are denoted by red arrows. (C) Micro Raman experimental results performed on monolayer, five-layer and bulk ReS_2 to show the out-of-plane vibrations of Re atoms. (D) Band structure of monolayer, trilayer and five-layer ReS_2 by *ab* initio calculations indicating band gaps of 1.44, 1.40 and 1.35 eV, respectively. (Reproduced from Ref. [121] with permission of Nature Publishing Group)

3.2.1 The preparation of TMDs

As we discussed above, mechanical cleavage, epitaxial growth, CVD and chemical method are the four major methods to prepare graphene 2D materials. TMDs are one of the 2D graphene analogues, which can also be produced by these methods. In order to explore the unique physicochemical properties that arise on reducing the thickness to single or few layers, scientists have developed appropriate ways to fabricate single-layer TMDs. For instance, scientists from Nanyang Technological University adopted mechanical cleavage method to strip out a 10 μm single-layer MoS_2 [122, 123] (Figure 7A). However, this method is expensive and time-consuming, and the mechanical exfoliation method introduces non-uniformity in the bulk crystals. To

feasibly control the thickness, shape, size, and position of the TMDs flakes, Steele et al utilized a laser to produce thinning multilayered MoS_2 down to a single-layer 2D crystal (Figure 7B) [123]. The laser-produced monolayers do not only possess fine semiconducting properties, but can also be tailored to arbitrary shapes and patterns in-process. Besides these, the transfer methods can also be applied for the preparation of layered TMDs. There are three common transfer methods: Wedging method, PVA method and Evalcite method. These three methods come with the same problems: the acceptor surface may contain structures sensitive to the chemicals used or to the capillary forces involved in the process. Therefore, scientists presented an all-dry transfer method, which relied on viscoelastic stamps and transferred 2D TMDs crystals without employing any wet chemistry to cause the capillary forces (Figure 7C and 7D) [124]. Recently, researchers from Tsinghua University developed an improved transfer method for the preparation of 2D TMDs (Figure 7E) [125].

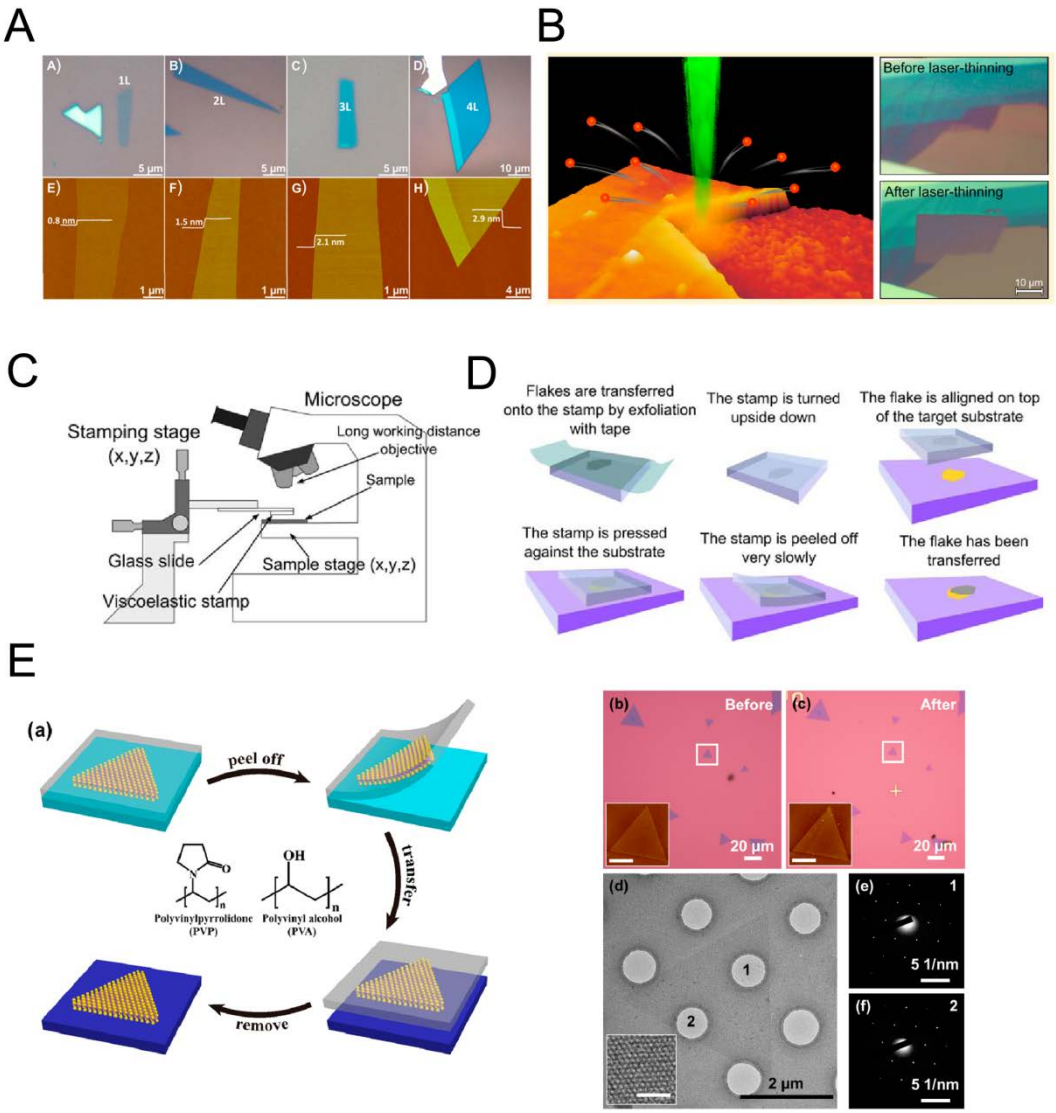

Figure 7 The three methods for the preparation of thin-layer TMDs. (A) Mechanically exfoliated single- and few-layer MoS_2 nanosheets on 300 nm SiO_2/Si. Optical microscopy (A-D) and AFM (E-H) images of MoS_2 nanosheets. (Reproduced from Ref. [122, 123] with permission of Wiley-VCH Verlag GmbH & Co). (B) Laser-produced monolayers method and optical microscopy image of a multilayered MoS_2 flake deposited onto a 285 nm SiO_2/Si substrate. (Reproduced from Ref. [123] with permission of American Chemical Society). (C-D) Schematic diagram of the all-dry transfer process. (Reproduced from Ref. [124] with permission of IOP Publishing 2014). (E) (a) Transfer of CVD-grown MoS_2 using the water-soluble bilayer polymer. (b, c) Optical and AFM images (insets) of CVD grown MoS_2 before and after transfer, respectively. (d) TEM image of a transferred MoS_2 flake on holey carbon grid. (e, f) SAED patterns taken on the area of MoS_2 flake marked with 1 and 2 in (d). (Reproduced from Ref. [125] with permission of American Chemical

Society).

3.2.2 Multi-functional TMDs based gene delivery systems

During the recent years, scientists have explored the potential of TMDs in biomedical applications due to their similar morphology and properties as graphene. In the TMDs family (including MoS_2, TaS_2, TiS_2, WS_2, ZrS_2, $NbSe_2$, WSe_2, Sb_2Se_3, and Bi_2Te_3), MoS2 attracts great interest in biomedical applications because Molybdenum is an essential trace element for several enzymes in cells and S is a common biological element. In 2013, for the first time, Zhang and co-workers revealed the high fluorescence quenching efficiency and different affinities of MoS_2 nanosheets toward ssDNA versus dsDNA, and used them as a sensing platform for the detection of DNA and small molecules [126]. The high absorbance profile of MoS_2 nanosheets enabled them to be heated up rapidly upon NIR irradiation and demonstrate better photothermal effects than graphene, which is considered as the current best-in-class NIR photothermal agent [127]. In subsequent studies, MoS_2 was functionalized with high biocompatibility and low cytotoxicity as drug or gene delivery systems for biomedical applications. For instance, Liu et al functionalized MoS_2 with folic acid (FA) and PEG to deliver chemotherapy drugs for cancer therapy. It was the first time when TMDs were applied as a novel type of 2D nano-carriers in drug delivery and cancer combination therapy [60]. Due to the negative charge of nucleic acid molecules, scientists have utilized the polyelectrolyte polymers (such as PEI) to modify MoS_2 nanosheets, which possess positive surface charge and provide promising potential for gene delivery (Figure 8A and 8B) [128, 129]. With the superior optical properties in NIR range, MoS_2-based nanocarriers could escape from

endosomal degradation by NIR irradiation and release the nucleic acid molecules in the cellular redox environment by redox reaction (Figure 8C).

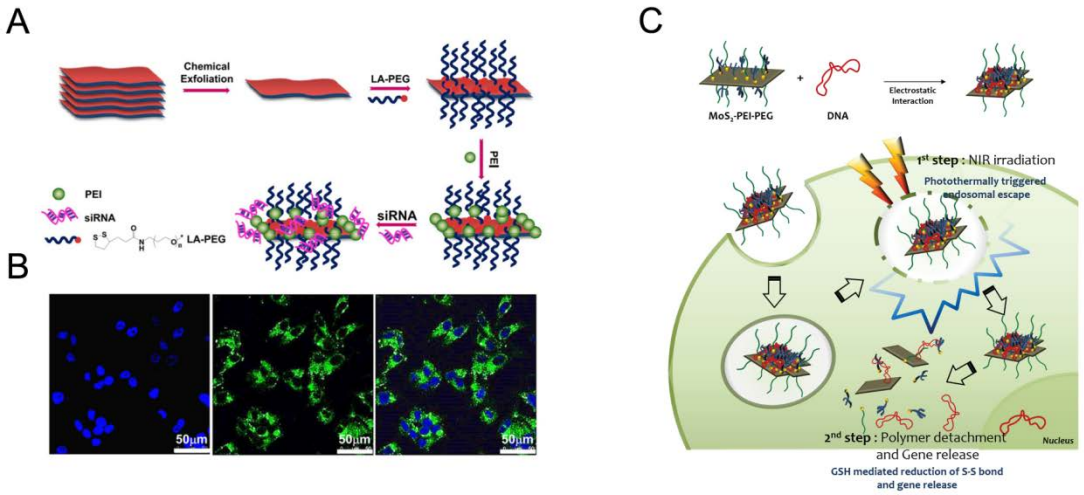

Figure 8 Gene delivery based on functional MoS_2 nanosheets. (A) Schematic illustration for the synthesis of siRNA loaded-MoS_2-PEG-PEI. (B) Confocal microscopy images of HepG2 cells (FAM-siRNA (green) and DAPI (blue)) confirm siRNA transfection after incubation with MoS_2–PEG–PEI/ FAM-siRNA for 4 h. (Reproduced from Ref. [128] with permission of BioMed Central Ltd 2014). (C) Schematic illustration of sequential plasmid DNA delivery using MoS_2–PEI–PEG nanocomposite through photothermally triggered endosomal escape. (Reproduced from Ref. [137] with permission of WILEY-VCH Verlag GmbH & Co. KGaA, Weinheim).

Besides the numerous biomedical applications of MoS_2, other TMDs such as $MoSe_2$, WS_2, WSe_2 and Bi_2Se_3 are also efficiently used for biosystems. For example, $MoSe_2$ nanosheets exfoliated and noncovalently modified by a facile PVP-assisted exfoliation method exhibited promising applications for biocompatible photothermal therapy (PTT) agents *in vitro*, which could also be encapsulated into a hydrogel matrix for certain intelligent devices [130]. Both multifunctional Bi_2Se_3 [131] and WS_2 [119] nanosheets showed strong absorbance in the NIR region for multimodal bio-imaging and highly effective photothermal ablation of tumors *in vivo*. WS_2 QDs,

synthesized uniformly with the combination of sonication and solvothermal treatment of bulk WS_2 at a mild temperature, exhibited strong fluorescence, good cell permeability, and low cytotoxicity in living cells, and demonstrated promising potential for *in vitro* and *in vivo* bioimaging [132]. As for the gene delivery systems, there are only limited reports for other TMDs except MoS_2 so far. The critical challenges for the further biomedical applications of TMDs are biodegradation and excretion issues [133]. Because of the highly crystallized structures, TMDs nanosheets are too integrative to degrade in physiological environment. Furthermore, the metal ions released from TMDs possess potential toxicity towards human bodies at elevated dosages. Therefore, the toxicity and metabolism are the critical issues which should be solved urgently for successful clinical applications.

3.3 Layered double hydroxides (LDHs)

Layered double hydroxides (LDHs) are a family of inorganic layered materials, also known as anionic clays, which consist of cationic brucite-like layers and exchangeable interlayer anions. In 1842, hydrotalcite was discovered in Sweden, which was the origination of LDHs. Until 1915, the exact formula of hydrotalcite, as reported by Manasse, was $[Mg_6Al_2(OH)_{16}]CO_3 \cdot 4H_2O$ [134]. In the subsequent years, scientists devoted great interests whereby they found the most divalent and trivalent cations with suitable anions that could form LDHs, which have positively charged layers of mixed metal hydroxides that require the presence of interlayer anions to maintain overall charge neutrality, with the generic formula as $[M^{2+}_{1-x}M^{3+}_{x}(OH)_2]^{x+}(A^{n-}_{f/n}) \cdot mH_2O$ (Figure 9A) [135, 136], where M^{2+} and M^{3+} denote divalent

and trivalent ions, A^{n-} denotes the interlayer exchangeable anions and *x* is molar ratio of trivalent cations in total cations (0.16~0.33). Due to the facile production, low cost and high biocompatibility, LDHs have been applied in wide areas, such as catalysis, adsorption and gene delivery. Nowadays, numerous kinds of LDHs are fabricated and applied in different fields. It is worth noting that the hydrolysis behavior in acidic media and anionic exchange capacity make LDHs as an ideal nanocarrier for drug and gene delivery (Figure 9B) [136, 137].

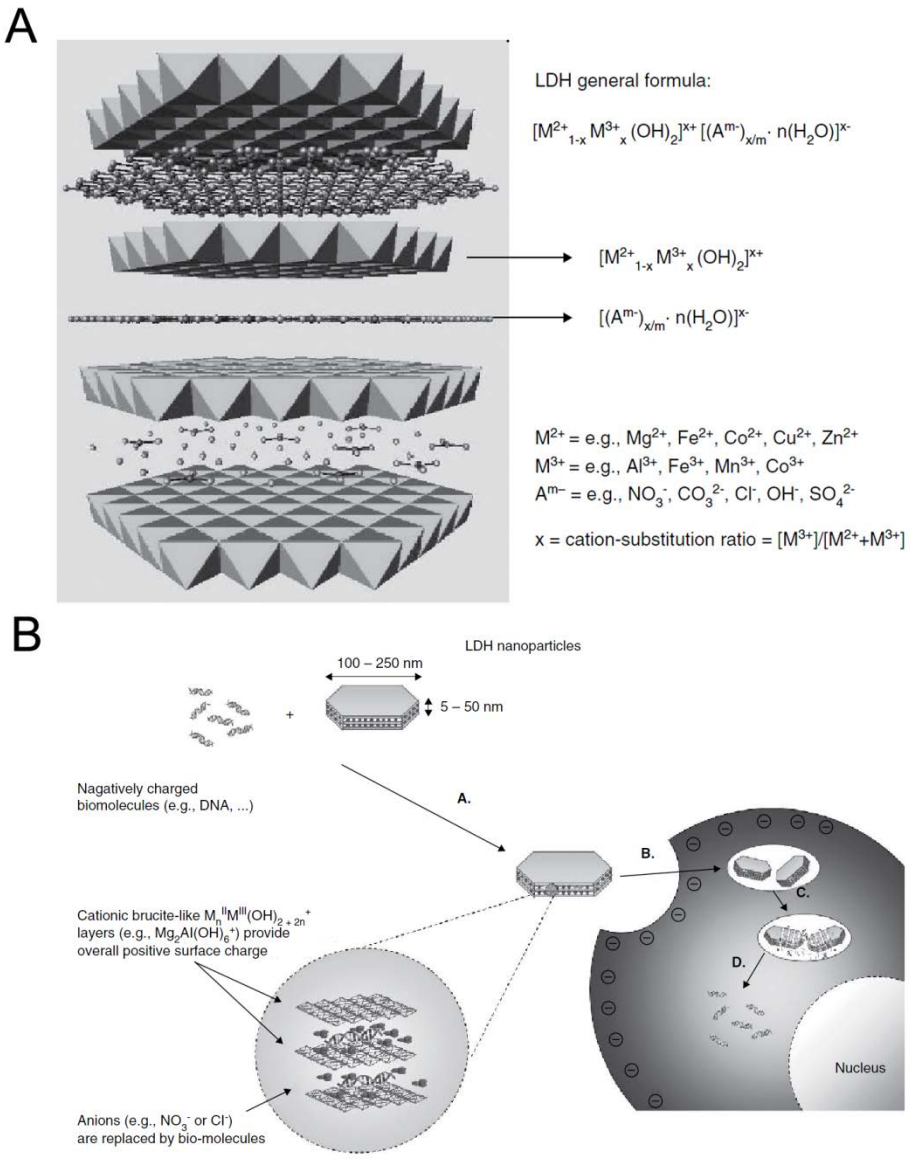

Figure 9 Structure of LDHs and gene delivery based on LDHs nanosheets in cells. (A) Schematic illustration showing the brucit-like layered structure of LDHs with negatively charged ions in the interlayer gallery for charge neutralization. (B) Schematic illustration of the mechanism for gene delivery based on LDHs in cells. (Reproduced from Ref.[136] with permission of Taylor & Francis 2009).

3.3.1 The preparation of LDHs

To date, there are four common methods for the preparation of LDHs: co-precipitation method, ion exchange method, calcination reconstruction method and hydrothermal method. The first three methods are widely used for LDHs synthesis and are discussed in details as follows.

(1) Co-precipitation method

Based on the specific experimental conditions, co-precipitation method can be divided into two strategies: 1) Constant pH co-precipitation method: A constant pH solution is prepared in accordance to the range of pH based on the co-precipitation of indicated metal ions, and then adding the alkali solution into the metal salt mixture solution dropwise to maintain a constant pH in the co-precipitation range [138, 139]. 2) Variable pH co-precipitation method: LDHs containing interlayer carbonate anions are prepared by adding a solution containing the desired divalent and trivalent metal cations to a solution of Na_2CO_3 until the pH of the reaction mixture reaches a specified value (typically around 10) and a solution of sodium hydroxide is then used to maintain the pH value until the precipitation is complete [140]. Constant pH co-precipitation method is more commonly used for the preparation of LDHs with uniform particle size.

(2) Ion exchange method

Although the co-precipitation method is the most widely used strategy for the preparation of LDHs, some specific conditions are inapplicable for co-precipitation method, such as the instability of the divalent or trivalent metal ions in alkaline solution, or the direct reaction between metal ions is more favorable. Therefore, ion exchange method is a suitable alternative, first reported by Bish [141]. Ion exchange method for LDHs depends on the electrostatic interactions between the positively-charged host sheets and the exchanging anions, in which the guests are exchanged with the anions present in the interlayer regions of preformed LDHs to

produce specific anion pillared LDHs [142, 143].

(3) Calcination reconstruction method

Calcination reconstruction method, also known as “calcination-rehydration process” or “structural memory effect”, is applied when the intercalated molecules are too large to be achieved by mechanical means, such as organic chromophores [144], surfactants [145], peptides [146] and hexose [147]. Based on the unique memory effect of LDHs, the lamellar structure of LDHs, which gets destroyed by calcining under the temperature ranging from 300 to 550 ºC, can be restored in water vapor or water solution with certain anions.

(4) Hydrothermal method

If the affinity of guest molecules is low and difficult to intercalate into the interlayers, hydrothermal method is the preferable strategy compared to anion-exchange reactions or co-precipitation. During the hydrothermal process, magnesium [148] and alumimium hydroxides [149] are the commonly used inorganic sources to ensure no other competing anions occupy the interlayer space [149]. Under different hydrothermal temperature, the crystal structures of the resulting material are different. An ordered structure can be obtained around 120 ºC, and a disordered one is formed at 100 ºC. Although the main layers of ordered and disordered structures are similar but the arrangements of water molecules and the interlayer region of composition formed by carbonate groups are different [149].

Besides these four common methods, other methods such as salt-oxide (or hydroxide) method [150], non-equilibrium aging method [151], non-conventional aging method

[152], surface synthesis [153], template synthesis [154] and sol-gel method [155] are available for the synthesis of special-purpose LDHs for different purposes.

3.3.2 Gene delivery based on LDHs nanosheets

To date, various kinds of nanoparticles are applied as gene delivery systems, including gold nanoparticles [156, 157], MSNs [158, 159], QDs [160, 161], polymeric micelles [162, 163] and liposomes [164, 165]. 2D nanomaterials have a much larger surface area per volume than other nanomaterials, which make them preferable gene nanocarriers with higher loading capacity. Due to the facile preparation, good biocompatibility, high loading capacity, tunable size and structure, pH-controlled release and refine protection cargo in the interlayer, LDHs are readily adaptable for gene delivery. In 1985, LDHs were applied to deliver nifedipine with sustained release for the first time, which paved the new era for applications of LDHs in biomedical fields [136]. In the next decades, scientists have devoted great research efforts on LDHs-based delivery systems. Chemotherapeutic drugs are one of the most common cargos delivered by LDHs, including γ-oxo-[1,1′-biphenyl]-4-butanoic acid (a non-steroidal anti-inflammatory drug) [166], methotrexate [167], Ibuprofen [168] and vitamin C [169] etc. In 1999, Choy et al utilized ion-exchange process to intercalate nucleic acid molecules into LDHs successfully [170]. Although nucleic acids are very susceptible to degradation and denaturation, they can be safely protected against strong alkaline and acidic environments even under the presence of Dnase/Rnase through intercalation into LDHs. In addition, LDHs exhibit negligible cytotoxicity, and are thus regarded as the ideal gene delivery system with high

biocompatibility. Besides single delivery studies, the co-delivery of siRNA and anti-cancer drugs have also been achieved by LDHs for cancer therapy. In the co-delivery system, both siRNA and anticancer drug 5-FU delivered by LDHs was controllably released and coordinately induced mitochondrial damage to overcome the drug resistance and enhance cancer treatment [171] (Figure 10). The uptake of nucleic acid molecules and drugs delivered by LDHs occurs via endocytosis, and then LDHs nanocarriers get dissolved under the low pH in the endosome, aiding nucleic acid molecules to escape into the cytoplasm [172, 173]. Besides these, other biological molecules such as amino acids and peptides [146], biocatalysts [174] and ATP [175] have also been delivered by LDHs. Table 2 lists the series of LDHs that have been reported as gene/drug delivery systems for biomedical applications (Table 2).

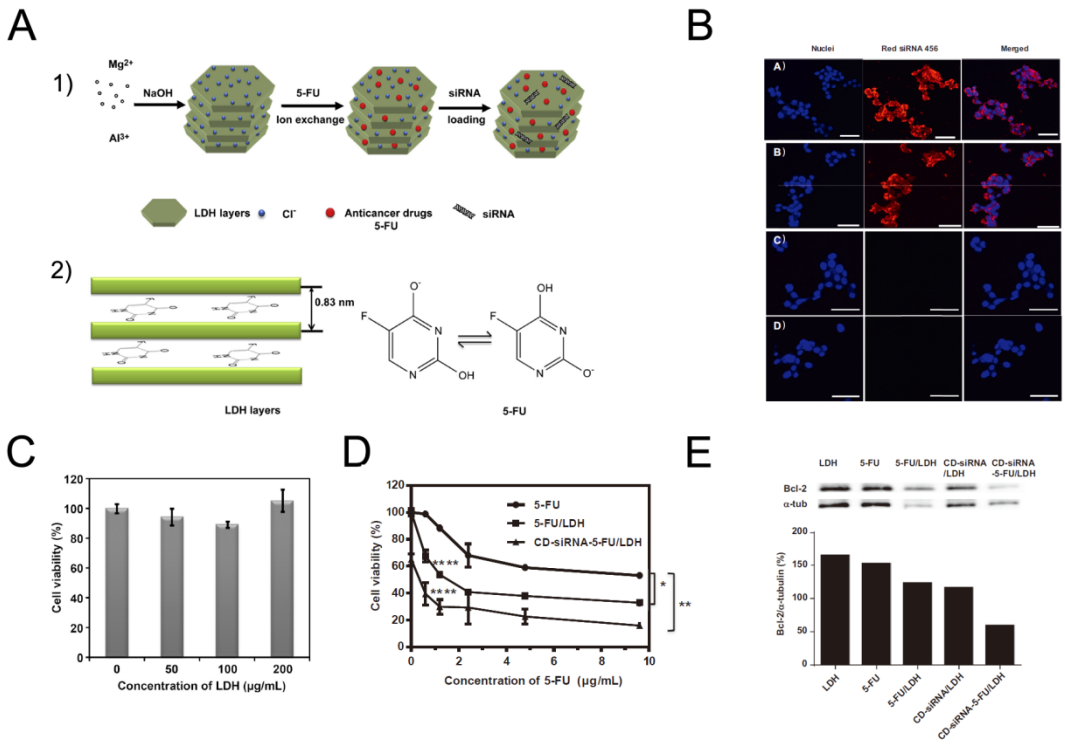

Figure 10 Co-delivery of siRNAs and anti-cancer drugs by LDHs for cancer therapy.

(A) Schematic diagram of the LDH co-delivery system to co-load 5-FU and siRNA (1) and schematic illustration of the horizontal laying of 5-FU in the interlayer (2). (B) Confocal microscopy images of MCF-7 cells taking up red siRNA 456/LDHs nanohybrids (A and C: cells cultured at 37 ºC and 4 ºC, respectively) and red siRNA 456-5-FU/LDHs nanocomplex (B and D: cells cultured at 37 ºC and 4 ºC, respectively). (C) Cytotoxicity of different concentrations LDHs to MCF-7 cell lines. (D) MTT assay analysis of effects of treatments with 5-FU, 5-FU(10)/LDH, CD-siRNA/LDHs, and CD-siRNA-5-FU/LDHs on the viability of MCF-7 cells at the 5-FU concentration from 0 to 9.6 mg/mL and the CD-siRNA concentration at 40 nM in all relevant treatments for 72 h. (E) Suppression of Bcl-2 protein expression in MCF-7 cells after single or combined treatment with 5-FU and CD-siRNA delivered by LDHs. (Reproduced from Ref. [171] with permission of 2014 Elsevier Ltd)

Table 2. Various LDH configurations used for drug delivery applications

Chemical composition	Interlayer anion	Cargo	Reference
MgAl-NO_3 LDHs	NO_3^-	Plasmid DNA	[137, 173, 176]
MgAl-NO_3 LDHs	NO_3^-	siRNA	[172, 177]
MgAl-Cl LDHs	Cl^-	Plasmid DNA	[178]
MgAl-Cl LDHs	Cl^-	Ibuprofen (IBU)	[168]
MgAl-CO_3 LDHs	CO_3^-	γ-oxo-[1,1V-biphenyl]-4-butanoic acid	[166]
LiAl-CO_3 LDHs	CO_3^-	γ-oxo-[1,1V-biphenyl]-4-butanoic acid	[166]
MgAl-NO_3 LDHs	NO_3^-	Methotrexate (MTX)	[167]
ZnFe–Cl LDHs	Cl^-	Vitamin C	[169]
MgFe–Cl LDHs	Cl^-	Vitamin C	[169]
MgAl-NO_3 LDHs	NO_3^-	Podophyllotoxin	[179]
ZnAl-NO_3 LDHs	NO_3^-	Benzoate derivatives (BzA)	[180]

3.4 Silicate clays

Due to the incomparable biosafety, silica materials are classified by the FDA as “Generally Recognized as Safe” (GRAS) and are widely used in food additives, cosmetics and pharmacy. Silicate clays are the most abundant and naturally available minerals on earth, which occupy a prominent status in drug products and are widely used both as excipients and active agents in drug products. During the last decades, silicate clays including montmorillonite, kaolinite and illite have been regarded as the

preferable drug delivery systems with good biocompatibility, high retention capacities, strong adsorption and ion exchange ability. Moreover, the swelling and colloidal properties endow clays with facile modulation for drug delivery. Protein and nucleic acids (DNA and RNA) can be adsorbed by silicate clays. As the synthetic procedures of silicate clays are similar as LDHs, we mainly focus on the gene delivery by silicate clays and the research progress during recent years in this part.

3.4.1 Mechanisms of interaction between silicate clays and nucleic acids

Due to the natural properties, ion exchange process is recognized as the most suitable approach for silicate clays to achieve drug controlled release (Figure 11A) [181]. The reversible interchange of ions with organic molecules by ion exchangers involves no qualitative change in the structure and properties of clays. Among the numerous kinds of silicates, montmorillonite and saponite that belong to smectites, are widely used for drug delivery. Besides ion exchange process, there are several other mechanisms, such as electrostatic interactions, hydrophobic affinity, hydrogen bonding and Van der Waals forces which are involved in the interaction between silicate clays and organic molecules.

For the adsorption of nucleic acids on silicate clays, ion exchange process is not suitable because of the specific structure and properties of nucleic acids. Therefore, other adsorption mechanisms including electrostatic forces, hydrogen bonding, ligand exchange and cation bridge have been explored. Electrostatic interaction method is the most widely used for binding negatively charged nucleic acid molecules and silicate clays. Chen et al studied the adsorption and desorption of salmon sperm DNA

on four different colloidal fractions from brown soil and clay minerals which indicated that the electrostatic force was the core way for the adsorption of nucleic acids on clay minerals. In comparison with ligand exchange, hydrogen bonding and cation bridge methods, electrostatic force is the most facile way to desorb nucleic acids from the surface of organic clays [182]. If some hydroxyl groups exist on the surface of silicate clays, ligand exchange is a suitable choice to interact with nucleic acids molecules by the reaction process between the phosphate groups at the two ends of the nucleic acid molecules which are directly bound to the hydroxyl group on the surface of clay minerals (Figure 11C) [183]. In addition to electrostatic forces and ligand exchange, multivalent cations in the medium contribute to the cation bridge process. The extent of DNA adsorption is affected by the concentration and valency of the cations, for example, the adsorption of nucleic acids is more efficient in the existence of Mg^{2+} and Ca^{2+} than in the existence of Na^{+} [184, 185]. The schemes of ligand exchange and cation bridge processes for DNA adsorption are depicted in Figure 11B and C. The cation bridge process strengthens the interaction between DNA and silicate clays to increase DNA stability and protect its degradation from enzymes [186].

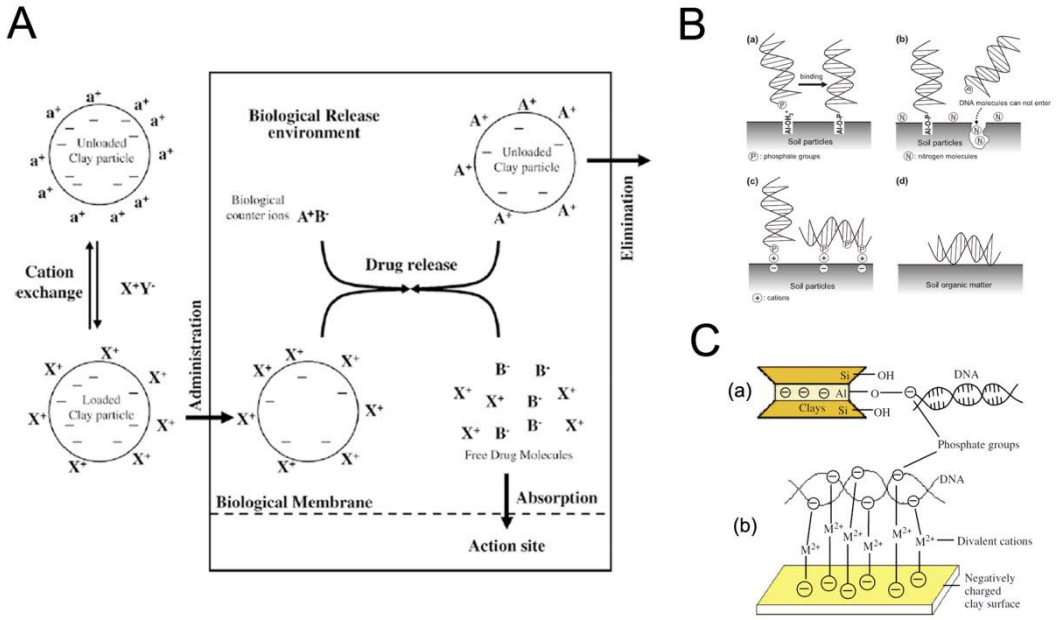

Figure 11 Schemes of different interactions between silicate clays and nucleic acids. (A) Clay–drug complexation and *in vivo* drug release mechanisms (clay mineral surface charge (−); compensating cations (a^+); cationic drug (X^+); drug associated anions (Y^-); *in vivo* counter ions (A^+); anions associated with the counter ions (B^-)). (Reproduced from Ref. [187] with permission of 2006 Elsevier B.V.) (B) Conceptual figures of DNA adsorption on the surface of silicate clays. (Reproduced from Ref. [183] with permission of Japanese Society of Microbial Ecology.) (C) Two interaction models of DNA and clay minerals; (a) Ligand exchange and (b) Cation bridge. (Reproduced from Ref. [186] with permission of 2013 Elsevier B.V.)

3.4.2 Factors influencing the interaction between silicate clays and nucleic acids

Although silicate clays have planar surface with a large area, the bonds formed between nucleic acids and external planar surface are weaker than the bonds between nucleic acids and edges of silicate clays [188]. To obtain efficient loading capacity, the structure and properties of silicate clays are essential factors which influence the amount of nucleic acids adsorption. For example, Cai and co-workers compared the ability of montmorillonite and kaolinite to bind with nucleic acids, and proved that the montmorillonite has the stronger binding ability [182]. Another silicate clay-illite, provided the lowest nucleic acids binding ability [189]. However, the results observed

with the existence of Ca^{2+} in silicate clays were different: Ca-illite > Ca-montmorillonite > Ca-kaolinite [190]. The structure and molecular weight of nucleic acids also affect the binding capacity of silicate clays. With the lower molecular weight of nucleic acids, the binding capacity of silicate clays (such as montmorillonite and kaolinite) increases [191]. In comparison with linear DNA, super-coiled plasmid DNA could overcome physical steric hindrances and subsequently be more efficient in interacting with silicate clays [190].

In addition to the former factors, the environment of solutions plays an important role on the adsorption of nucleic acids by silicate clays. Due to the isoelectric point of DNA (pI ≈ 5), the protonation of the amino groups of adenine, guanine and cytosine occurs below pH5, which induces nucleic acids adsorption on both internal and external surface of silicate clays. Cai et al studied the adsorption of DNA by silicate clays and found the decrease of DNA adsorption followed by the increase pH of solution from 2 to 5 [192]. Above pH5, the protonation would be suppressed while the negatively charged DNA molecules (due to the phosphate groups) can only be absorbed on the external surface of silicate clays by electrostatic interaction. Moreover, the existence of inorganic cations (e.g. Na^{+}, Ca^{2+} and K^{+}) in solutions are conductive to the formation of cation bridge between nucleic acids and silicate clays. Generally, the DNA adsorption is more efficiently enhanced by divalent cations (e.g. Mg^{2+} and Ca^{2+}) than monovalent cations (e.g. K^{+} and Na^{+}). Based on the above studies, numerous factors are involved in the DNA adsorption by silicate clays, which should be comprehensively considered for the efficient loading.

3.4.3 Use of silicate clays as gene delivery systems for biomedical applications

Silicate clays possess incomparable biosafety as gene delivery systems for biomedical applications. In the last decade, silicate clays have attracted great attention in gene delivery. Besides the biosafety, they possess additional excellent merits for gene delivery. First, the nucleic acids adsorption by silicate clays exhibits structural stability to protect nucleic acids degradation from the rigorous conditions, such as highly acidic or alkaline environments, the presence of DNA/RNA enzyme and even ultraviolet radiation treatment [186, 189, 193]. Second, the facilely functionalized surface of silicate clays can achieve targeting transfection for different therapeutic aims. For instance, Kuo and co-workers modified montmorillonite by intercalating the cationic hexadecyltrimethylammonium (HDTMA) for intercalation into the interlayer and served as a layer expander for higher DNA adsorption [194]. In the first report to show the DNA protective effect of silicate clays as oral gene delivery system, Kiyohito Yagi et al utilized sodium montmorillonite as a nanocarrier to deliver plasmid DNA into cells of small intestine, which showed potent DNA protection from the acidic environment in the stomach and DNA-degrading enzymes in the intestine. Moreover, compared to viral vectors, silicate clays based gene delivery system avoid severe immunological and toxicological responses and are thus considered as safe and high efficiency vectors for gene therapy [186, 195].

3.5 Transition metal oxides (TMOs)

As compared with other atomically thin materials, TMOs such as MnO_2, MoO_3, WO_3, Ga_2O_3, and V_2O_5 have a relatively longer history. In TMOs, the transition *s*

electrons are pulled by oxygen while the physical and chemical properties are mainly determined by the strongly correlated *d* electrons. Due to the diversity of the chemical composition and relative ease in inducing oxygen defect, TMO nanosheet show remarkable electronic properties and unique optical, mechanical and thermal phenomena [196]. Perovskites are another large family of 2D TMOs, which have the general formula of ABO_3 in which A ion is located in the corner of the cubic cell while B ion is transition metal ion at the center of the cubic cell as shown in Figure 12.

Based on the unique physical and chemical properties, the 2D TMOs are used in lithium batteries, supercapacitors, energy storage, fuel cells, diagnosis and theranostics.

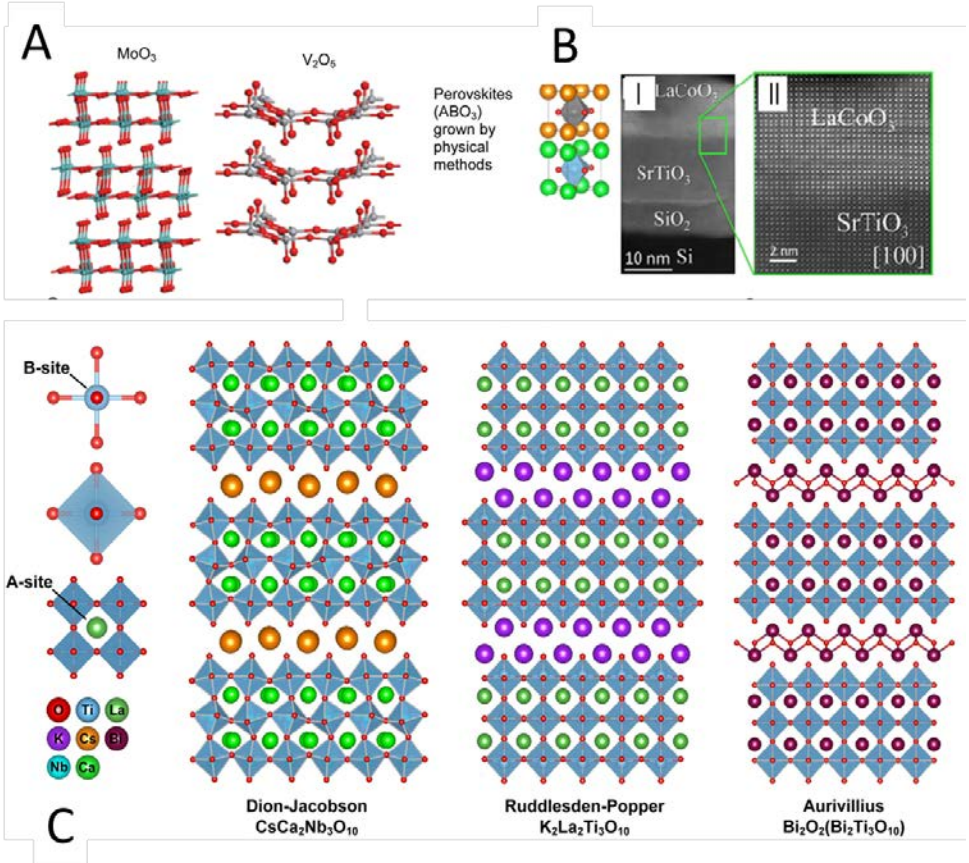

Figure 12. Representatives of 2D TMOs and their selected characteristics. (A) Layered α-MoO_3 and V_2O_5. (B) Cross-sectional high angle annular dark field scanning transmission electron microscopy image of ultra-thin films of perovskites epitaxially grown on silicon substrate by MBE (I) and enlarged view of the interface (II). (C) Different layered perovskites. Reproduced from Ref. [196] with permission of 2014 Elsevier Ltd.

3.5.1 The preparation of TMOs

In gas phase process, the flux of adatoms and the lowest unfilled surface energy of the substrate determine the quality of the layer-by-layer oxide epitaxy of TMOs. The thin-film growth can also be controlled at the unit-cell level using in site real-time reflection high-energy electron diffraction (RHEED) monitoring [197]. In this case, one or a few unit cells can be grown. The commonly used vapor phase techniques include molecular beam epitaxy (MBE), pulsed laser deposition (PLD), atomic layer deposition (ALD) and CVD. Mechanical exfoliation is another well-known method to form thin 2D TMOs from their stratified crystals. However, mechanical exfoliation using sticky tapes has limited yield and is only suitable for laboratory research works. Exfoliation can also be done in liquid phase. The intercalant can be inserted to increase the separation between the planes followed by the exfoliation of the layers. In this case, electrostatic repulsion and expansion of interlayer entities are normally used to realize the chemical exfoliation. Furthermore, vigorous ultrasonication can also be used for direct exfoliation of stratified TMOs.

3.5.2 Multi-functional TMOs based gene delivery systems

As the typical 2D TMOs, MnO_2 nanosheets are extensively used in biological applications [198-200]. First, the MnO_2 nanosheets can strongly adsorb ssDNA and drug by physisorption; second, MnO_2 nanosheets can be reduced to Mn^{2+} ions by

intracellular glutathione (GSH), then the generated Mn^{2+} ions act as efficient cofactors of 10-23 DNAzyme for gene silencing. Moreover, the reduction of MnO_2 nanosheets provides active magnetic resonance and fluorescence signaling. Thus, MnO_2 nanosheets are vital nanocarriers for delivering DNAzyme drug into the cell for cancer therapy.

Chen constructed a theranostic platform based on chemically exfoliated 2D MnO_2 nanosheets for pH-responsive MRI and drug release [199]. Upon entering the acidic microenvironment of tumor tissue, the functionalized MnO_2 nanosheet is quickly broken up. Such pH-responsive behavior promotes fast release of the loaded anticancer drug for chemotherapy. Meanwhile, the released Mn^{2+} ions can be used as the MRI agent for high-performance tumor imaging and detection. Fan proposed a DNAzyme-MnO_2 nanosystem for efficient gene-silencing therapy [198]. As shown in Figure 13, the Ce6-labelled DNAzyme can provide gene silencing, PDT and fluorescence imaging, whereas MnO_2 nanosheet acts as the nanocarrier for Ce6-labelled DNAzyme, serves as a potential provider of cofactor (Mn^{2+}) for 10-23 DNAzyme and as an active MRI contrast agent. Once endocytosed, Mn^{2+} ions are generated due to the reduction of MnO_2 nanosheets by intracellular GSH, thus leading to 10-23 DNAzyme cleavage to target RNA. The therapeutic efficacy is further enhanced by the photodynamic effect of Ce6 under visible light irradiation. Meanwhile the fluorescence/MRI signal can be used to estimate the delivery efficiency.

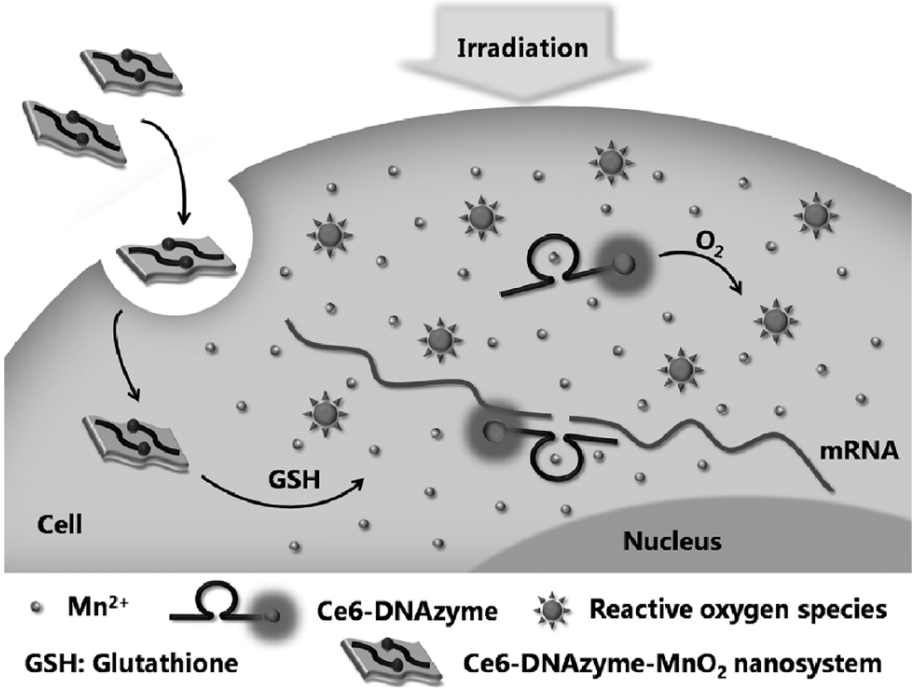

Figure 13. Activated mechanism of the Ce6-DNAzyme-MnO_2 nanosystem for gene silencing and PDT. (Reproduced from Ref. [198] with permission of Wiley-VCH Verlag GmbH & Co).

3.6 Black phosphorus (BP)

As a new member of 2D materials, atomically thin BP has generated new opportunities for innovatively electronic and biomedical applications [201-203]. As a metal-free layered semiconductor, BP nanosheet exhibits a tunable thickness-dependent bandgap (from 0.3 eV for bulk to 2.0 eV for single layer), meanwhile its accurate optical response and anisotropic charge transport can be achieved by modifying the structure, thereby enabling fascinating electronic and photoelectronic applications. Recently, BP has been used in field-effect transistor, thin film solar cell and gas sensing. Phosphorus is considered as a crucial element in the human body as it amounts to approximately 660 g in an adult human and accounts for about 1% of the body weight. Besides that, the experiments have shown that BP could react with water and oxygen, and then degraded in aqueous media. Moreover, the

final degradation products are nontoxic phosphate and phosphonate [204]. The good biocompatibility and biodegradation makes BP a promising therapeutic agent. Due to its quite high surface to volume ratio, BP has large drug loading capacity, enhancing the therapeutic efficiency. By virtue of its unique electronic structure, BP is a highly efficient photosensitizer [205] and used to generate singlet oxygen in photodynamic treatment. In addition, the BP shows a broad absorption across the entire ultraviolet to the near-infrared (NIR) regions [206], making it a suitable choice for photothermal treatment.

3.6.1 The preparation of BP

Mechanical exfoliation technique is to prepare the BP atomic layers, similar to the method used to prepare other atomically thin 2D materials, but this method is only suitable for laboratory level demonstrations. Recently the liquid exfoliation method has been proposed and become the commonly utilized method to prepare BP nanosheets with different thicknesses and sizes for bioimaging and phototherapy applications [206, 207].

As shown in Fig. 14, BP has the corrugated plane of P atoms that are connected by strong intra-layer P-P bonding and weak inter-layer Van der Waals forces. Thus, it is possible for bulk BP to be exfoliated into thin BP nanosheets with a few layers or even a monolayer by breaking down the weak inter-layer interactions. The BP nanosheets can be prepared using the simple liquid exfoliation technique involving ultrasound probe sonication followed by bath sonication of ground powders of bulk BP as shown in Figure 14. Many reports about the exfoliation of BP in organic

solvents have been published. However, the organic solvents that were used for exfoliation of BP were easily adsorbed on the surface of the BP, which need to be removed prior to use for biological applications [208]. Recently, the bulk BP could be exfoliated into ultrathin nanosheets in water via a simple water exfoliation strategy as shown in Figure 14C, and the exfoliated BP nanosheets were more promising in biological applications. The morphology of the exfoliated BP nanosheets is shown in Figure 14. The thickness and size of the exfoliated BP could be modified by the liquid exfoliation conditions.

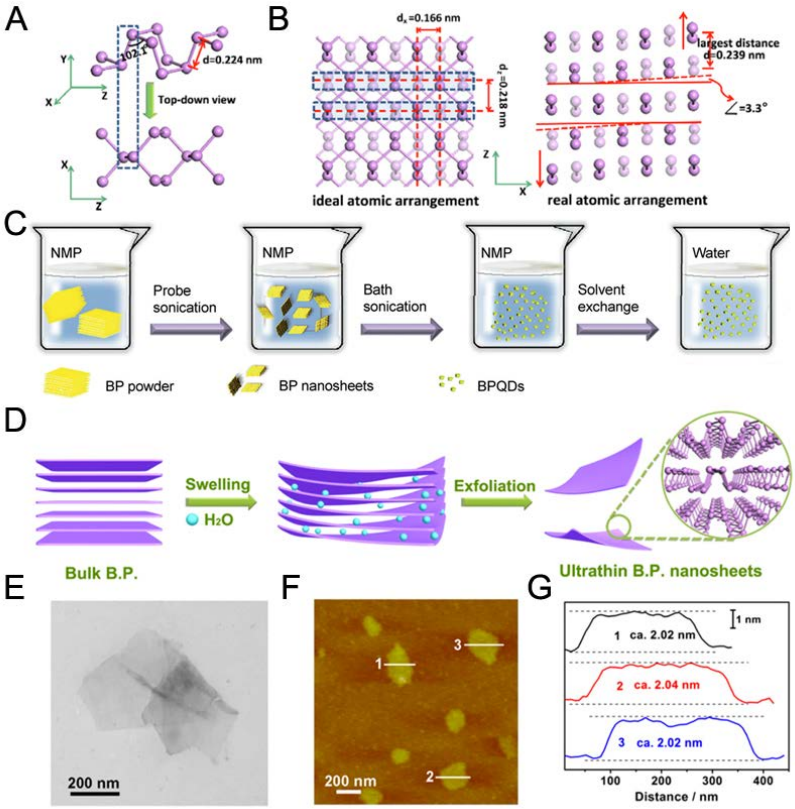

Figure 14. (A) Structure of B.P. projected along different directions. (B) Schematic illustration of the ideal and real atomic arrangement of the multilayered B.P. nanosheets (Reproduced from Ref. [205] with permission of American Chemical Society). Schematic illustration for the (C) water exfoliation (Reproduced from Ref. [203] with permission of Wiley-VCH Verlag GmbH & Co) and (D) organic solvent exfoliation of bulk BP into ultrathin nanosheets. (E) TEM image. (F) AFM image. (G)

Corresponding height image of BP nanosheets (Reproduced from Ref. [205] with permission of American Chemical Society).

3.6.2 Multi-functional BP based gene delivery systems

In comparison with other 2D materials, BP has a much higher surface to volume ratio due to its puckered lattice configuration as shown in Fig.15a, which increases its drug loading capacity. Meanwhile, due to its unique electronic characteristics, BP can be used as a highly efficient photosensitizer for PDT applications. In addition, the absorption of BP can cover the entire visible range enabling the NIR photothermal properties for PTT treatments. All these unique properties of BP make it an optimum drug delivery platform for multimodal therapy of cancer.

Sun synthesized the BP quantum dots (BPQDs) for PTT applications, which showed excellent NIR photothermal performance with large extinction coefficient, photothermal conversion efficiency and good photostability [206]. After PEG conjugation and incubation with cells, the *in vitro* experimental results showed that the nanoparticles were a good photothermal agent. Shao encapsulated the BPQDs with poly(lactic-co-glycolic acid) (PLGA) loaded by an emulsion method to form biodegradable nanospheres [209]. The hydrophobic PLGA can isolate the oxygen and water to enhance the photothermal stability of BP and control the degradation rate. The *in vitro* and *in vivo* experiments demonstrate that the BPQDs/PLGA nanospheres have minimal cytotoxicity, good biocompatibility and excellent PTT efficiency.

As the key component in PDT, traditional photosensitizer suffers from low singlet oxygen species (ROS) quantum yields and lack of long wavelength absorption band. BP provides a new possibility to overcome these shortcomings. The exfoliated BP

nanosheets are demonstrated to be a good PDT agent with the ROS quantum yield of about 0.91 under the 660 nm laser excitation [205]. *In vitro* and *in vivo* experimental results have shown notable cancer therapy ability of BP nanosheets. To further move the excitation wavelength to the NIR range and improve the PDT efficiency, the upconversion nanoparticles (UCNPs) are integrated into the BP system, which generate visible light (650 nm) under the NIR excitation (808 nm) [210]. Under NIR irradiation, the composite exhibits excellent antitumor efficiency due to the large amount of ROS generated by BP nanosheets.

Recently, the BP based drug delivery system for synergistic imaging, PDT, PTT or chemotherapy of cancer has also been proposed and demonstrated [211, 212]. Figure 16 illustrates the schematic procedure of the fabricated BP-based drug delivery system. It was found that a large amount of DOX (950% in weight) could be loaded onto the BP nanosheet surface, meanwhile the BP nanosheet could generate enough ROS and heat for PDT and PTT treatment. The proposed system showed the pH-/ photoresponsive drug release properties, wherein DOX was released under the acidic tumor biological environment and the release was further accelerated under the NIR laser irradiation due to the photothermal effect of BP nanosheet. Shown in Fig. 15 c-e, we reported the engineering of polyelectrolyte polymers coated BPQDs-based nanocarriers to deliver siRNA in human ovarian teratocarcinoma PA-1 cells. It was the first application of BPQDs nanodots as gene delivery systems, which showed the promising potential for siRNA delivery and photothermal effect without cytotoxicity for cancer therapy.

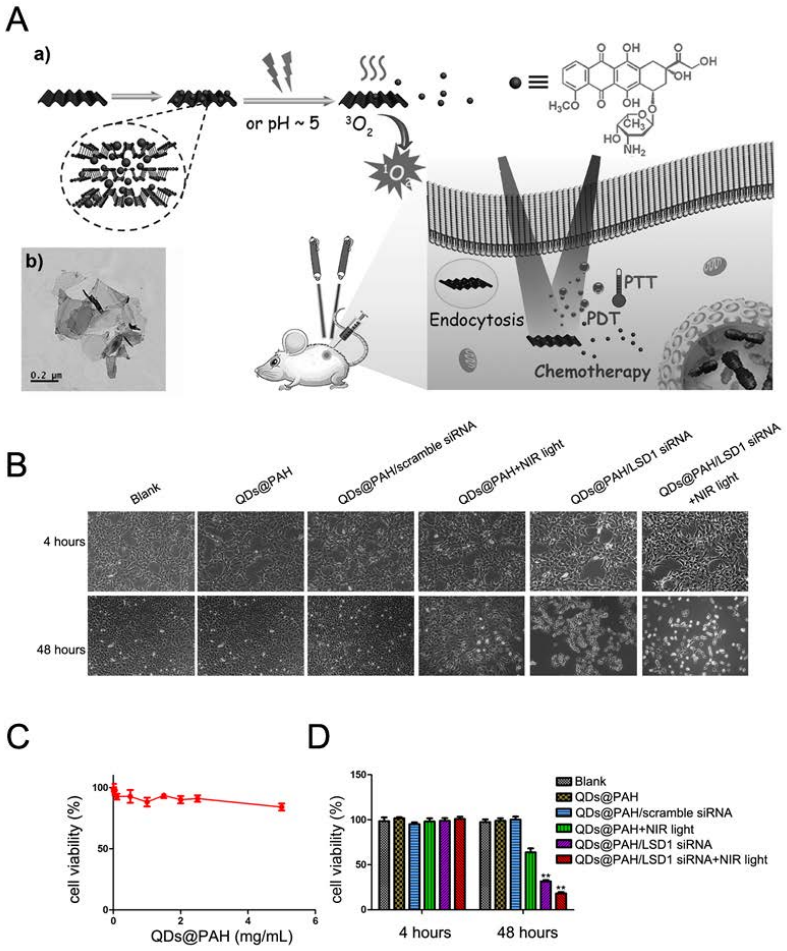

Figure 15. (A) Schematic illustration of BP-based drug delivery system for synergistic therapy of cancer. (B) TEM image of BP nanosheets. (Reproduced from Ref.[211] with permission of Wiley-VCH Verlag GmbH & Co). (C-E) Cell viability tests of different BP-QDs nanocomplexes with NIR light. The growth of PA-1 cells (cultured in 6-well plate) was inhibited distinctly by BP-QDs@PAH/siRNA nanocomplex with NIR light (under review).

4. Conclusions and Perspectives

This review summarized the latest progress and achievements of gene delivery by functionalized 2D nanomaterials, including Graphene and GO, TMDs, LDHs, silicate clays, TMOs and BP. These rapidly emerging carbon based 2D nanomaterials and graphene analogues (such as TMDs, BP, etc.), possess specific planar morphology and physicochemical properties, making them effective in imaging, drug delivery, diagnosis and therapy. Although these 2D nanomaterials have distinguished

advantages, they also have some limitations for gene delivery application, which are summarized in Table 3. Hence, careful evaluation of these factors can aid to make an optimum choice for the selecting a specific 2D nanomaterial for gene delivery applications. Other 2D nanomaterials, for e.g. metal organic frameworks (MOFs) have been reported to be served as gene/drug delivery system with efficient delivery, but lack *in vivo* toxicity reports for further applications [213, 214]. Examples of these nanomaterials for gene delivery applications are not summarized in this review. Up to now, the biological applications using 2D nanomaterials are still in the early stage, but many groups including our group have attempted to exploit their advanced gene delivery and synergistic treatment modalities wherein promising results have been achieved. In our recent studies, we have developed three kinds of gene delivery systems: FA/PEG/GO, FA/PEG/MoS_2 and BP-QDs/PAH. With low-toxicity, biocompatibility high loading efficiency and photothermal properties, FA/PEG/GO [110] and FA/PEG/MoS_2 delivery systems both exhibited promising potential in targeted gene therapy and photothermal effect for pancreatic cancer treatments. As the first application of BP-QDs as gene delivery systems, we demonstrated BP-QDs/PAH promising potentials for siRNA delivery and photothermal effect in cancer therapy *in vitro*. Furthermore, because phosphorus is an essential element in the body, BP in the physiological environment will be oxidized and reduced into nontoxic phosphate ions and phosphite ions, and this fact could support its applications for clinical trial. Lastly, it is important to devise a rule of thumb for selecting the appropriate 2D nanomaterial for gene delivery. The following guidelines should be adopted while selecting the

appropriate 2D nanomaterial for effective therapeutic outcomes: (i) Prior cytotoxicity studies must be performed before their use for in vivo applications. The overall concentration of all 2D nanomaterials used for the studies should be compared. The lower the concentration, the better it is; (ii) the toxicity assessment of the functionalization agents should also be done. For instance, PEI, which is a commonly used functionalization agent, should be used in a reduced amount of concentration for attaching gene molecules because it is quite toxic; (iii) The overall hydrodynamic diameter of the 2D nanomaterials must be minimized so that they can have longer blood circulation time for gene delivery application; (iv) One should also attach specific ligands or homing agents to the surface of the 2D nanomaterials for targeted delivery to the infected sites such as cancer and diseased cells; (v) The kinetic release profile of the gene molecules should also be studied carefully for formulating the best nanoplex for effective gene delivery therapy.

Table 3. An overview of various 2D nanomaterials for gene delivery applications

2D material	Multifunctionalized forms	Specific gene delivery application	Advantages	Disadvantages
Graphene oxide	GO-PEI	plasmid DNA delivery into mammalian cell lines and zebrafish embryos [215]	- High loading efficiency - Facile surface functionalization - Tunable size and structure - Good biocompatibility - Protected delivery - Superior optical properties in NIR range for photothermal effect.	- The aggregation of GO in liver and other organs is hard to be metabolized - GO can evoke strong aggregator response in human platelets and trigger extensive pulmonary thromboembolism [216].
		mRNA delivery in cells to mediate generation of "footprint-free" iPSCs [104]		
	GO-PEG-PEI	plasmid DNA delivery into Drosophila S2 cells [217]		
	GO-CS	plasmid DNA delivery [99]		
	GO-PEI-PSS	co-delivery of anti-cancer drugs and microRNA in breast cancer MCF7 cells, effective in drug-resistant tumor cells [109]		
	FA/PEG/PAH modified GO	*in vivo* cancer targeting and siRNA delivery (Unpublished data)		
	GO-gold nanoparticles-PEI	DNA delivery [111]		
	pSiNPs-GO	high level of siRNA loading, slow release of siRNA [218]		
Transition metal dichalcogenides	MoS_2-FA-PEG	Drug delivery for cancer therapy [219]	- High loading efficiency - Protected delivery - Superior optical properties in NIR range for bio-imaging and photothermal effect.	- Due to the highly crystallized structures, TMDs are hard to be degraded in vivo - The metal ions of TMDs may exhibit potential toxicity
	MoS_2-PEG-PEI	siRNA delivery in HepG2 cells [128]		
		sequential plasmid DNA delivery[113]		

Layered double hydroxides	$MgAl-NO_3$ LDHs	co-delivery of siRNA and anti-cancer drug 5-FU [220]	- Facile preparation - Good biocompatibility - High loading capacity - Tunable size and structure - Protected delivery - Controlled release	- Unstable chemical properties of LDHs - Uncontrollable release of nucleic acids intercalated in LDHs - Unstable interactions between cargos and LDHs for in vivo applications.
	$MgAl-NO_3$ LDHs	Plasmid DNA [221] [222, 223]		
	$MgAl-NO_3$ LDHs	siRNA [172, 224]		
	MgAl-Cl LDHs	Plasmid DNA [178]		
Silicate clays	Montmorillonite-HDTMA	DNA adsorption and delivery [194]	- Protected delivery - Controlled release - Good biocompatibility	- The size of delivery cargos is limited due to the limitation of interlayer spacing of silicate clays - Release from silicate clays varies uncontrollably - Hard to be degraded and metabolized in vivo
	sodium montmorillonite	plasmid DNA delivery into cells of small intestine [195]		
Transition metal oxides (TMOs)	MnO_2 nanosheets	DNAzyme drug delivery into the cell [198]	- Facile surface functionalization - High compatibility to avoid severe immunological and toxicological responses - Controllable release by pH - Generated ions (e.g. Mn2+) can act as cofactors.	- The bond formed between nucleic acids and external planar surface are weaker than that between nucleic acids and edges of silicate clays, which limits the delivery efficiency - Hard to be degraded and metabolized in vivo.
	MnO_2 nanosheets	pH-responsive MRI and drug release [225]		
Black phosphorus	PEG-BPQDs	PTT applications [206]	- High ROS quantum yield as a	- The fast oxidization in air

	BPQDs/PLGA nanospheres	PTT applications [209]	good PDT agent - Superior optical properties in NIR range for photothermal effect - Highest loading efficiency - Good biocompatibility - BPs get oxidized and then reduce to nontoxic phosphate and phosphonate in the physiological environment	induces extremely unstable structure of BP and limit their further applications.
	UCNPs-BP nanosheets	PDT agents for cancer therapy [210]		
	DOX/BP nanosheet	pH-/photoresponsive drug delivery [211]		
	PAH/BP-QDs nanocomplexes	siRNA delivery in human ovarian teratocarcinoma PA-1 cells (Unpublished data)		

The use of 2D nanomaterials in gene delivery and other biomedicine applications are very exciting and promising, there are a lot of unresolved critical issues nonetheless that need to be addressed by systematic investigations:

1) The preparation methods of 2D nanomaterials: Various methods such as mechanical exfoliation method, liquid exfoliation method, etc. are used for the preparation of 2D nanomaterials, yet a standard control to achieve nanosheets or nanodots with the desired structure such as size, dispersity, hydrophilicity and surface functionalities is not defined. All the above-mentioned parameters are critical factors to determine the practical therapeutic/diagnostic effects using the as-prepared 2D nanomaterials, and thus the fabrication approach needs to be standardized and optimized.

2) The functionalization of 2D nanomaterials: Most 2D nanomaterials for biomedicine applications are prepared using liquid exfoliation method, and sometimes the organic solvents are used. To improve their biocompatibility, hydrophilicity and stability in biological environment, some biocompatible and hydrophilic polymers like PEG are used for encapsulation. Some 2D nanomaterials like BP can quickly and easily degrade in aqueous medium which limits the practical biomedical applications and makes the PEGylation a necessity to isolate the oxygen and aqueous solution. Therefore, the PEGylation or other encapsulation process should be investigated and optimized to achieve better therapeutic or diagnostic effects. In addition, there is significant accumulation of these 2D nanomaterials in the reticuloendothelial system due to the lack of targeting specificities. Thus, the surface engineering of the 2D

nanomaterials with targeted functionalization enables the 2D nanomaterials to accumulate at the specific site in order to enhance the therapeutic or diagnostic performance and relieve the side-effects.

3) The biosafety aspect of using 2D nanomaterials: It is necessary and mandatory to investigate the impact of using these 2D nanomaterials on health and environment before they can be employed for practical applications. Since the study on the emerging 2D nanomaterials is still at the initial stage, there is limited data of their *in vitro* and *in vivo* toxicity. More detailed investigations of the long-term toxicity of these 2D nanomaterials are necessary and essential. Furthermore, the toxicity assessment of these 2D nanomaterials should be inclusive of but not restricted to the biodistribution, biodegradation, excretion and potential toxic effects to specific organs, including neurotoxicity, reproductive toxicity and the influences on embryonic development. It is well known that the toxicities may have different results when used with different cell lines and animal models. Thus, it is necessary to update the animal models to the large ones such as pig or primates when evaluating the potential clinical possibility of 2D nanomaterials.

The properties of 2D nanomaterials are distinct, enabling them to be attractive nano-agents for gene delivery and other biomedical applications. Encouragingly, the current results have proven 2D nanomaterials as a promising nanosystem that could provide a new opportunity to promote the new generation of multi-modal therapy and imaging which are difficult to fulfill using the traditional strategies. Two critical issues that will need to be addressed before the practical clinical use of 2D

nanomaterials are the long-term toxicity and environmental persistence. Considering the short history and rapid development of 2D nanomaterials in biological applications, we foresee viable solutions to their biosafety and pharmaceutical issues so that the biological applications of 2D nanomaterials can ultimately benefit human health.

Acknowledgements

This study was supported by the Ministry of Education, Singapore (Tier 2 MOE2010-T2-2-010), NTU-NHG Innovation Collaboration Grant, A*STAR Science and Engineering Research Council, NTU-A*STAR Silicon Technologies, Centre of Excellence program grant, NEWRI Seed Grant, the Research Grants Council (RGC) of Hong Kong (Project Nos. PolyU 153030/15P and 153271/16P) and School of Electrical and Electronic Engineering at Nanyang Technological University..

References

[1] R.L. Siegel, K.D. Miller, A. Jemal, Ca-Cancer J Clin, 66 (2016) 7-30.
[2] G. Taroncher-Oldenburg, Science-Business eXchange, 2 (2009) 1-4.
[3] M. Collins, A. Thrasher, Proceedings. Biological sciences / The Royal Society, 282 (2015) 20143003.
[4] M.A. Kay, Nature reviews. Genetics, 12 (2011) 316-328.
[5] S.A. Rosenberg, P. Aebersold, K. Cornetta, A. Kasid, R.A. Morgan, R. Moen, E.M. Karson, M.T. Lotze, J.C. Yang, S.L. Topalian, M.J. Merino, K. Culver, A.D. Miller, R.M. Blaese, W.F. Anderson, New Engl J Med, 323 (1990) 570-578.
[6] M.G. Ott, M. Schmidt, K. Schwarzwaelder, S. Stein, U. Siler, U. Koehl, H. Glimm, K. Kuhlcke, A. Schilz, H. Kunkel, S. Naundorf, A. Brinkmann, A. Deichmann, M. Fischer, C. Ball, I. Pilz, C. Dunbar, Y. Du, N.A. Jenkins, N.G. Copeland, U. Luthi, M. Hassan, A.J. Thrasher, D. Hoelzer, C. von Kalle, R. Seger, M. Grez, Nat Med, 12 (2006) 401-409.
[7] S.E. Boye, S.L. Boye, A.S. Lewin, W.W. Hauswirth, Mol Ther, 21 (2013) 509-519.
[8] H.B. Gaspar, Blood, 120 (2012) 3628-3629.
[9] W.G. Wierda, M.J. Cantwell, S.J. Woods, L.Z. Rassenti, C.E. Prussak, T.J. Kipps, Blood, 96 (2000) 2917-2924.
[10] R.T. Bartus, M.S. Weinberg, R.J. Samulski, Mol Ther, 22 (2014) 487-497.
[11] T. Zhang, Curr Drug Deliv, 11 (2014) 233-242.
[12] N. Nayerossadat, T. Maedeh, P.A. Ali, Advanced biomedical research, 1 (2012) 27.
[13] R.J. Cristiano, Anticancer Res, 18 (1998) 3241-3245.

[14] P.D. Robbins, S.C. Ghivizzani, Pharmacol Therapeut, 80 (1998) 35-47.
[15] Y. Yi, M.J. Noh, K.H. Lee, Curr Gene Ther, 11 (2011) 218-228.
[16] W.S.M. Wold, K. Toth, Curr Gene Ther, 13 (2013) 421-433.
[17] E.A. Burton, D.J. Fink, J.C. Glorioso, DNA Cell Biol, 21 (2002) 915-936.
[18] Z.S. Guo, D.L. Bartlett, Expert Opin Biol Th, 4 (2004) 901-917.
[19] O. Mazda, Curr Gene Ther, 2 (2002) 379-392.
[20] D.M. Shayakhmetov, A. Gaggar, S. Ni, Z.Y. Li, A. Lieber, Journal of virology, 79 (2005) 7478-7491.
[21] G.T. Mercier, J.A. Campbell, J.D. Chappell, T. Stehle, T.S. Dermody, M.A. Barry, Proceedings of the National Academy of Sciences of the United States of America, 101 (2004) 6188-6193.
[22] H. Miyoshi, U. Blomer, M. Takahashi, F.H. Gage, I.M. Verma, Journal of virology, 72 (1998) 8150-8157.
[23] L. Vannucci, M. Lai, F. Chiuppesi, L. Ceccherini-Nelli, M. Pistello, The new microbiologica, 36 (2013) 1-22.
[24] D. Stone, A. David, F. Bolognani, P.R. Lowenstein, M.G. Castro, The Journal of endocrinology, 164 (2000) 103-118.
[25] M. Ramamoorth, A. Narvekar, Journal of clinical and diagnostic research : JCDR, 9 (2015) GE01-06.
[26] X.R. You, Y. Kang, G. Hollett, X. Chen, W. Zhao, Z.P. Gu, J. Wu, J Mater Chem B, 4 (2016) 7779-7792.
[27] N. Qiu, L. Cai, W. Wang, G. Wang, X. Cheng, Q. Xu, J. Wen, J. Liu, Y. Wei, L. Chen, Journal of Inclusion Phenomena and Macrocyclic Chemistry, 82 (2015) 505-514.
[28] H.L. Gao, Q.Y. Zhang, Z.Q. Yu, Q. He, Curr Pharm Biotechno, 15 (2014) 210-219.
[29] L. Cai, X. Wang, W. Wang, N. Qiu, J. Wen, X. Duan, X. Li, X. Chen, L. Yang, Z. Qian, Y. Wei, L. Chen, International journal of nanomedicine, 7 (2012) 4499-4510.
[30] P. Harvie, F.M.P. Wong, M.B. Bally, J Pharm Sci, 89 (2000) 652-663.
[31] J.Y. Legendre, A. Trzeciak, B. Bohrmann, U. Deuschle, E. Kitas, A. Supersaxo, Bioconjugate Chem, 8 (1997) 57-63.
[32] S.J. Son, X. Bai, S.B. Lee, Drug Discov Today, 12 (2007) 650-656.
[33] Z.P. Xu, Q.H. Zeng, G.Q. Lu, A.B. Yu, Chem Eng Sci, 61 (2006) 1027-1040.
[34] A.L. Bailey, P.R. Cullis, Biochemistry-Us, 36 (1997) 1628-1634.
[35] J.Y. Legendre, A. Trzeciak, B. Bohrmann, U. Deuschle, E. Kitas, A. Supersaxo, Bioconjugate Chem, 8 (1997) 57-63.
[36] H.X. Wang, W. Chen, H.Y. Xie, X.Y. Wei, S.Y. Yin, L. Zhou, X. Xu, S.S. Zheng, Chem Commun, 50 (2014) 7806-7809.
[37] T.R. Kuang, Y.R. Liu, T.T. Gong, X.F. Peng, X.L. Hu, Z.Q. Yu, Curr Nanosci, 12 (2016) 38-46.
[38] E. Phillips, O. Penate-Medina, P.B. Zanzonico, R.D. Carvajal, P. Mohan, Y.P. Ye, J. Humm, M. Gonen, H. Kalaigian, H. Schoder, H.W. Strauss, S.M. Larson, U. Wiesner, M.S. Bradbury, Sci Transl Med, 6 (2014).
[39] J. Perez-Juste, I. Pastoriza-Santos, L.M. Liz-Marzan, P. Mulvaney, Coordin

Chem Rev, 249 (2005) 1870-1901.
[40] S.D. Huo, S.B. Jin, K.Y. Zheng, S.T. He, D.L. Wang, X.J. Liang, Chinese Sci Bull, 58 (2013) 4072-4076.
[41] C.M. Yu, L.H. Qian, J.Y. Ge, J.Q. Fu, P.Y. Yuan, S.C.L. Yao, S.Q. Yao, Angew Chem Int Edit, 55 (2016) 9272-9276.
[42] C.M. Yu, L.H. Qian, M. Uttamchandani, L. Li, S.Q. Yao, Angew Chem Int Edit, 54 (2015) 10574-10578.
[43] S.C. McBain, H.H. Yiu, J. Dobson, International journal of nanomedicine, 3 (2008) 169-180.
[44] M. Arruebo, R. Fernández-Pacheco, M.R. Ibarra, J. Santamaría, Nano Today, 2 (2007) 22-32.
[45] C.E. Probst, P. Zrazhevskiy, V. Bagalkot, X.H. Gao, Adv Drug Deliver Rev, 65 (2013) 703-718.
[46] R.D.K. Misra, Nanomedicine-Uk, 3 (2008) 271-274.
[47] K.S. Novoselov, A.K. Geim, S.V. Morozov, D. Jiang, Y. Zhang, S.V. Dubonos, I.V. Grigorieva, A.A. Firsov, Science, 306 (2004) 666-669.
[48] D. Chimene, D.L. Alge, A.K. Gaharwar, Adv Mater, 27 (2015) 7261-7284.
[49] Y. Chen, C.L. Tan, H. Zhang, L.Z. Wang, Chem Soc Rev, 44 (2015) 2681-2701.
[50] X.D. Zhuang, Y.Y. Mai, D.Q. Wu, F. Zhang, X.L. Feng, Adv Mater, 27 (2015) 403-427.
[51] K.J. Koski, Y. Cui, Acs Nano, 7 (2013) 3739-3743.
[52] H. Zhang, Acs Nano, 9 (2015) 9451-9469.
[53] S. Bai, Y.J. Xiong, Sci Adv Mater, 7 (2015) 2168-2181.
[54] B. Mendoza-Sanchez, Y. Gogotsi, Adv Mater, 28 (2016) 6104-6135.
[55] L. Wang, Q. Xiong, F. Xiao, H. Duan, Biosensors & bioelectronics, (2016).
[56] Y. Chen, C. Tan, H. Zhang, L. Wang, Chem Soc Rev, 44 (2015) 2681-2701.
[57] L. Feng, Z. Liu, Nanomedicine (Lond), 6 (2011) 317-324.
[58] C.J. Wu, A.K. Gaharwar, P.J. Schexnailder, G. Schmidt, Materials, 3 (2010) 2986-3005.
[59] S.J. Choi, J.H. Choy, Nanomedicine-Uk, 6 (2011) 803-814.
[60] T. Liu, C. Wang, X. Gu, H. Gong, L. Cheng, X.Z. Shi, L.Z. Feng, B.Q. Sun, Z. Liu, Adv Mater, 26 (2014) 3433-3440.
[61] K. Shavanova, Y. Bakakina, I. Burkova, I. Shtepliuk, R. Viter, A. Ubelis, V. Beni, N. Starodub, R. Yakimova, V. Khranovskyy, Sensors-Basel, 16 (2016).
[62] V. Nicolosi, M. Chhowalla, M.G. Kanatzidis, M.S. Strano, J.N. Coleman, Science, 340 (2013) 1420-+.
[63] V. Tran, R. Soklaski, Y.F. Liang, L. Yang, Phys Rev B, 89 (2014).
[64] Y.T. Zhao, H.Y. Wang, H. Huang, Q.L. Xiao, Y.H. Xu, Z.N. Guo, H.H. Xie, J.D. Shao, Z.B. Sun, W.J. Han, X.F. Yu, P.H. Li, P.K. Chu, Angew Chem Int Edit, 55 (2016) 5003-5007.
[65] H. Shen, L.M. Zhang, M. Liu, Z.J. Zhang, Theranostics, 2 (2012) 283-294.
[66] H. Fernandezmoran, J Appl Phys, 31 (1960) 1840-1840.
[67] H.P. Boehm, A. Clauss, G.O. Fischer, U. Hofmann, Z Anorg Allg Chem, 316 (1962) 119-127.

[68] F. Bonaccorso, A. Lombardo, T. Hasan, Z.P. Sun, L. Colombo, A.C. Ferrari, Mater Today, 15 (2012) 564-589.
[69] H. Tetlow, J.P. de Boer, I.J. Ford, D.D. Vvedensky, J. Coraux, L. Kantorovich, Phys Rep, 542 (2014) 195-295.
[70] Y. Zhang, L.Y. Zhang, C.W. Zhou, Accounts Chem Res, 46 (2013) 2329-2339.
[71] S. Park, R.S. Ruoff, Nat Nanotechnol, 4 (2009) 217-224.
[72] M. Yi, Z.G. Shen, J Mater Chem A, 3 (2015) 11700-11715.
[73] A.V. Zaretski, D.J. Lipomi, Nanoscale, 7 (2015) 9963-9969.
[74] J.S. Wu, L. Gherghel, M.D. Watson, J.X. Li, Z.H. Wang, C.D. Simpson, U. Kolb, K. Mullen, Macromolecules, 36 (2003) 7082-7089.
[75] S. Stankovich, D.A. Dikin, R.D. Piner, K.A. Kohlhaas, A. Kleinhammes, Y. Jia, Y. Wu, S.T. Nguyen, R.S. Ruoff, Carbon, 45 (2007) 1558-1565.
[76] Y. Yurum, B.S. Okan, F. Okyay, A. Yurum, F. Dinc, N. Gorgulu, S.A. Gursel, Key Eng Mater, 543 (2013) 9-12.
[77] W.S. Hummers, R.E. Offeman, J Am Chem Soc, 80 (1958) 1339-1339.
[78] B.J. Hong, O.C. Compton, Z. An, I. Eryazici, S.T. Nguyen, Acs Nano, 6 (2012) 63-73.
[79] Y. Zhang, T.R. Nayak, H. Hong, W. Cai, Nanoscale, 4 (2012) 3833-3842.
[80] C. Chung, Y.K. Kim, D. Shin, S.R. Ryoo, B.H. Hong, D.H. Min, Acc Chem Res, 46 (2013) 2211-2224.
[81] J.B. Liu, Y.L. Li, Y.M. Li, J.H. Li, Z.X. Deng, J Mater Chem, 20 (2010) 900-906.
[82] H. Guo, X. He, J. Zhong, Q. Zhong, Q. Leng, C. Hu, J. Chen, L. Tian, Y. Xi, J. Zhou, Journal of Materials Chemistry A, 2 (2014) 2079-2087.
[83] W.B. Hu, C. Peng, M. Lv, X.M. Li, Y.J. Zhang, N. Chen, C.H. Fan, Q. Huang, Acs Nano, 5 (2011) 3693-3700.
[84] R. Kanchanapally, B.P.V. Nellore, S.S. Sinha, F. Pedraza, S.J. Jones, A. Pramanik, S.R. Chavva, C. Tchounwou, Y. Shi, A. Vangara, D. Sardar, P.C. Ray, Rsc Adv, 5 (2015) 18881-18887.
[85] H.B. Wang, Q. Zhang, X. Chu, T.T. Chen, J. Ge, R.Q. Yu, Angew Chem Int Edit, 50 (2011) 7065-7069.
[86] B.A. Chen, M. Liu, L.M. Zhang, J. Huang, J.L. Yao, Z.J. Zhang, J Mater Chem, 21 (2011) 7736-7741.
[87] L.M. Zhang, Z.X. Lu, Q.H. Zhao, J. Huang, H. Shen, Z.J. Zhang, Small, 7 (2011) 460-464.
[88] Y.Z. Piao, T.F. Wu, B.Q. Chen, Ind Eng Chem Res, 55 (2016) 6113-6121.
[89] E.Y. Choi, T.H. Han, J.H. Hong, J.E. Kim, S.H. Lee, H.W. Kim, S.O. Kim, J Mater Chem, 20 (2010) 1907-1912.
[90] S.J. Liu, Q. Wen, L.J. Tang, J.H. Jiang, Anal Chem, 84 (2012) 5944-5950.
[91] P.Y. Li, K.Y. Cheng, X.C. Zheng, P. Liu, X.J. Xu, Funct Mater Lett, 9 (2016).
[92] (!!! INVALID CITATION !!! [106, 107]).
[93] M. Fang, K.G. Wang, H.B. Lu, Y.L. Yang, S. Nutt, J Mater Chem, 19 (2009) 7098-7105.
[94] C.S. Shan, H.F. Yang, D.X. Han, Q.X. Zhang, A. Ivaska, L. Niu, Langmuir, 25 (2009) 12030-12033.

[95] E. Doustkhah, S. Rostamnia, J Colloid Interf Sci, 478 (2016) 280-287.
[96] Y.P. Chen, Y.Y. Qi, B. Liu, J Nanomater, (2013).
[97] H.J. Salavagione, M.A. Gomez, G. Martinez, Macromolecules, 42 (2009) 6331-6334.
[98] J. Zhang, L.Z. Feng, X.F. Tan, X.Z. Shi, L.G. Xu, Z. Liu, R. Peng, Part Part Syst Char, 30 (2013) 794-803.
[99] H.Q. Bao, Y.Z. Pan, Y. Ping, N.G. Sahoo, T.F. Wu, L. Li, J. Li, L.H. Gan, Small, 7 (2011) 1569-1578.
[100] J.Q. Dalagan, E.P. Enriquez, B Mater Sci, 37 (2014) 589-595.
[101] M.L. Chen, J.W. Liu, B. Hu, M.L. Chen, J.H. Wang, Analyst, 136 (2011) 4277-4283.
[102] T.N. Lambert, C.A. Chavez, B. Hernandez-Sanchez, P. Lu, N.S. Bell, A. Ambrosini, T. Friedman, T.J. Boyle, D.R. Wheeler, D.L. Huber, J Phys Chem C, 113 (2009) 19812-19823.
[103] X. Zhou, F. Laroche, G.E.M. Lamers, V. Torraca, P. Voskamp, T. Lu, F.Q. Chu, H.P. Spaink, J.P. Abrahams, Z.F. Liu, Nano Res, 5 (2012) 703-709.
[104] H.Y. Choi, T.J. Lee, G.M. Yang, J. Oh, J. Won, J. Han, G.J. Jeong, J. Kim, J.H. Kim, B.S. Kim, S.G. Cho, Journal of Controlled Release, 235 (2016) 222-235.
[105] V.V. Namboodiri, R.S. Varma, Green Chem, 3 (2001) 146-148.
[106] J.H. Park, G. Saravanakumar, K. Kim, I.C. Kwon, Adv Drug Deliver Rev, 62 (2010) 28-41.
[107] Y. Wu, H. Luo, H. Wang, C. Wang, J. Zhang, Z. Zhang, J Colloid Interface Sci, 394 (2013) 183-191.
[108] Y. Xu, H. Bai, G. Lu, C. Li, G. Shi, J Am Chem Soc, 130 (2008) 5856-5857.
[109] F. Zhi, H. Dong, X. Jia, W. Guo, H. Lu, Y. Yang, H. Ju, X. Zhang, Y. Hu, PLoS One, 8 (2013) e60034.
[110] F. Yin, K. Hu, Y. Chen, M. Yu, D. Wang, Q. Wang, K.T. Yong, F. Lu, Y. Liang, Z. Li, Theranostics, 7 (2017) 1133-1148.
[111] C. Xu, D.R. Yang, L. Mei, B.G. Lu, L.B. Chen, Q.H. Li, H.Z. Zhu, T.H. Wang, Acs Appl Mater Inter, 5 (2013) 2715-2724.
[112] J. Joo., E.J. Kwon., J. Kang., M. Skalak., E.J. Anglin., A.P. Mann., E. Ruoslahti., S.N. Bhatia., M.J. Sailor., Nanoscale Horizons, 1 (2016) 407-414.
[113] E. Liu, Y. Fu, Y. Wang, Y. Feng, H. Liu, X. Wan, W. Zhou, B. Wang, L. Shao, C.H. Ho, Y.S. Huang, Z. Cao, L. Wang, A. Li, J. Zeng, F. Song, X. Wang, Y. Shi, H. Yuan, H.Y. Hwang, Y. Cui, F. Miao, D. Xing, Nature communications, 6 (2015) 6991.
[114] B.W. Baugher, H.O. Churchill, Y. Yang, P. Jarillo-Herrero, Nat Nanotechnol, 9 (2014) 262-267.
[115] S. Larentis, B. Fallahazad, E. Tutuc, Appl Phys Lett, 101 (2012).
[116] M.R. Gao, Y.F. Xu, J. Jiang, S.H. Yu, Chem Soc Rev, 42 (2013) 2986-3017.
[117] J. Yang, D. Voiry, S.J. Ahn, D. Kang, A.Y. Kim, M. Chhowalla, H.S. Shin, Angew Chem Int Edit, 52 (2013) 13751-13754.
[118] T. Liu, C. Wang, W. Cui, H. Gong, C. Liang, X. Shi, Z. Li, B. Sun, Z. Liu, Nanoscale, 6 (2014) 11219-11225.
[119] L. Cheng, J.J. Liu, X. Gu, H. Gong, X.Z. Shi, T. Liu, C. Wang, X.Y. Wang, G.

Liu, H.Y. Xing, W.B. Bu, B.Q. Sun, Z. Liu, Adv Mater, 26 (2014) 1886-1893.
[120] M. Pumera, A.H. Loo, Trac-Trend Anal Chem, 61 (2014) 49-53.
[121] E.F. Liu, Y.J. Fu, Y.J. Wang, Y.Q. Feng, H.M. Liu, X.G. Wan, W. Zhou, B.G. Wang, L.B. Shao, C.H. Ho, Y.S. Huang, Z.Y. Cao, L.G. Wang, A.D. Li, J.W. Zeng, F.Q. Song, X.R. Wang, Y. Shi, H.T. Yuan, H.Y. Hwang, Y. Cui, F. Miao, D.Y. Xing, Nature communications, 6 (2015).
[122] H. Guo, J. Chen, L. Tian, Q. Leng, Y. Xi, C. Hu, ACS Applied Materials & Interfaces, 6 (2014) 17184-17189.
[123] A. Castellanos-Gomez, M. Barkelid, A.M. Goossens, V.E. Calado, H.S.J. van der Zant, G.A. Steele, Nano Lett, 12 (2012) 3187-3192.
[124] A. Castellanos-Gomez, M. Buscema, R. Molenaar, V. Singh, L. Janssen, H.S.J. van der Zant, G.A. Steele, 2d Mater, 1 (2014).
[125] Z.X. Lu, L.F. Sun, G.C. Xu, J.Y. Zheng, Q. Zhang, J.Y. Wang, L.Y. Jiao, Acs Nano, 10 (2016) 5237-5242.
[126] C.F. Zhu, Z.Y. Zeng, H. Li, F. Li, C.H. Fan, H. Zhang, J Am Chem Soc, 135 (2013) 5998-6001.
[127] S.S. Chou, B. Kaehr, J. Kim, B.M. Foley, M. De, P.E. Hopkins, J. Huang, C.J. Brinker, V.P. Dravid, Angew Chem Int Edit, 52 (2013) 4160-4164.
[128] Z.Y. Kou, X. Wang, R.S. Yuan, H.B. Chen, Q.M. Zhi, L. Gao, B. Wang, Z.J. Guo, X.F. Xue, W. Cao, L. Guo, Nanoscale Res Lett, 9 (2014).
[129] J. Kim, H. Kim, W.J. Kim, Small, 12 (2016) 1184-1192.
[130] Z.Y. Lei, W.C. Zhu, S.J. Xu, J. Ding, J.X. Wan, P.Y. Wu, Acs Applied Materials & Interfaces, 8 (2016) 20900-20908.
[131] J. Li, F. Jiang, B. Yang, X.R. Song, Y. Liu, H.H. Yang, D.R. Cao, W.R. Shi, G.N. Chen, Sci Rep-Uk, 3 (2013).
[132] S.J. Xu, D. Li, P.Y. Wu, Adv Funct Mater, 25 (2015) 1127-1136.
[133] Y. Chen, L.Z. Wang, J.L. Shi, Nano Today, 11 (2016) 292-308.
[134] A.I. Khan, D. O'Hare, J Mater Chem, 12 (2002) 3191-3198.
[135] Z.P. Xu, G.S. Stevenson, C.Q. Lu, G.Q.M. Lu, P.F. Bartlett, P.P. Gray, J Am Chem Soc, 128 (2006) 36-37.
[136] K. Ladewig, Z.P. Xu, G.Q. Lu, Expert Opin Drug Del, 6 (2009) 907-922.
[137] J.H. Choy, S.Y. Kwak, Y.J. Jeong, J.S. Park, Angew Chem Int Edit, 39 (2000) 4042-4045.
[138] L. Lv, J. He, M. Wei, D.G. Evans, Z.L. Zhou, Water Res, 41 (2007) 1534-1542.
[139] E.M. Seftel, E. Popovici, M. Mertens, K. Witte, G. Tendeloo, P. Cool, E.F. Vansant, Micropor Mesopor Mat, 113 (2008) 296-304.
[140] D.G. Evans, D.A. Xue, Chem Commun, (2006) 485-496.
[141] D.L. Bish, B Mineral, 103 (1980) 170-175.
[142] M. Meyn, K. Beneke, G. Lagaly, Inorg Chem, 29 (1990) 5201-5207.
[143] S.V. Prasanna, P.V. Kamath, Ind Eng Chem Res, 48 (2009) 6315-6320.
[144] G.G. Aloisi, U. Costantino, F. Elisei, L. Latterini, C. Natali, M. Nocchetti, J Mater Chem, 12 (2002) 3316-3323.
[145] Y.W. You, H.T. Zhao, G.F. Vance, J Mater Chem, 12 (2002) 907-912.
[146] H. Nakayama, N. Wada, M. Tsuhako, Int J Pharm, 269 (2004) 469-478.

[147] S. Aisawa, H. Hirahara, S. Takahashi, Y. Umetsu, E. Narita, Chem Lett, 33 (2004) 306-307.
[148] Z.P. Xu, G.Q. Lu, Chem Mater, 17 (2005) 1055-1062.
[149] M. Ogawa, S. Asai, Chem Mater, 12 (2000) 3253-+.
[150] E.L. Crepaldi, P.C. Pavan, J.B. Valim, J Brazil Chem Soc, 11 (2000) 64-70.
[151] L. Huang, D.Q. Li, D.G. Evans, X. Duan, Eur Phys J D, 34 (2005) 321-323.
[152] R. Galindo, A. Lopez-Delgado, I. Padilla, M. Yates, Appl Clay Sci, 95 (2014) 41-49.
[153] O.C. Wilson, T. Olorunyolemi, A. Jaworski, L. Borum, D. Young, A. Siriwat, E. Dickens, C. Oriakhi, M. Lerner, Appl Clay Sci, 15 (1999) 265-279.
[154] E. Geraud, S. Rafqah, M. Sarakha, C. Forano, V. Prevot, F. Leroux, Chem Mater, 20 (2008) 1116-1125.
[155] M.A. Aramendia, V. Borau, U. Jimenez, J.M. Marinas, J.R. Ruiz, F.J. Urbano, J Solid State Chem, 168 (2002) 156-161.
[156] D. Pissuwan, T. Niidome, M.B. Cortie, J Control Release, 149 (2011) 65-71.
[157] P. Nishtha, Y. Chengbin, Y. Feng, Y. Ho Sup, C. Tjin Swee, Y. Ken-Tye, Nanotechnology, 26 (2015) 365101.
[158] I.I. Slowing, J.L. Vivero-Escoto, C.W. Wu, V.S.Y. Lin, Adv Drug Deliver Rev, 60 (2008) 1278-1288.
[159] F. Torney, B.G. Trewyn, V.S.Y. Lin, K. Wang, Nat Nanotechnol, 2 (2007) 295-300.
[160] M.V. Yezhelyev, L.F. Qi, R.M. O'Regan, S. Nie, X.H. Gao, J Am Chem Soc, 130 (2008) 9006-9012.
[161] W.B. Tan, S. Jiang, Y. Zhang, Biomaterials, 28 (2007) 1565-1571.
[162] N. Nishiyama, K. Kataoka, Pharmacol Therapeut, 112 (2006) 630-648.
[163] T.G. Park, J.H. Jeong, S.W. Kim, Adv Drug Deliver Rev, 58 (2006) 467-486.
[164] N.S. Templeton, D.D. Lasic, Mol Biotechnol, 11 (1999) 175-180.
[165] Y. Liu, L.C. Mounkes, H.D. Liggitt, C.S. Brown, I. Solodin, T.D. Heath, R.J. Debs, Nat Biotechnol, 15 (1997) 167-173.
[166] B.X. Li, J. He, D.G. Evans, X. Duan, Appl Clay Sci, 27 (2004) 199-207.
[167] J.H. Choy, J.S. Jung, J.M. Oh, M. Park, J. Jeong, Y.K. Kang, O.J. Han, Biomaterials, 25 (2004) 3059-3064.
[168] A.C.S. Alcantara, P. Aranda, M. Darder, E. Ruiz-Hitzky, J Mater Chem, 20 (2010) 9495-9504.
[169] M.S. Gasser, Colloid Surface B, 73 (2009) 103-109.
[170] J.H. Choy, S.Y. Kwak, J.S. Park, Y.J. Jeong, J. Portier, J Am Chem Soc, 121 (1999) 1399-1400.
[171] L. Li, W.Y. Gu, J.Z. Chen, W.Y. Chen, Z.P. Xu, Biomaterials, 35 (2014) 3331-3339.
[172] K. Ladewig, M. Niebert, Z.P. Xu, P.P. Gray, G.Q.M. Lu, Biomaterials, 31 (2010) 1821-1829.
[173] K. Ladewig, M. Niebert, Z.P. Xu, P.P. Gray, G.Q. Lu, Appl Clay Sci, 48 (2010) 280-289.
[174] M.B.A. Rahman, M. Basri, M.Z. Hussein, M.N.H. Idris, R.N.Z.R.A. Rahman,

A.B. Salleh, Catal Today, 93-5 (2004) 405-410.
[175] H. Tamura, J. Chiba, M. Ito, T. Takeda, S. Kikkawa, Solid State Ionics, 172 (2004) 607-609.
[176] A. Li, L.L. Qin, W.R. Wang, R.R. Zhu, Y.C. Yu, H. Liu, S.L. Wang, Biomaterials, 32 (2011) 469-477.
[177] Y.Y. Wong, K. Markham, Z.P. Xu, M. Chen, G.Q. Lu, P.F. Bartlett, H.M. Cooper, Biomaterials, 31 (2010) 8770-8779.
[178] Z.P. Xu, T.L. Walker, K.L. Liu, H.M. Cooper, G.Q.M. Lu, P.F. Bartlett, International journal of nanomedicine, 2 (2007) 163-174.
[179] L.L. Qin, M. Xue, W.R. Wang, R.R. Zhu, S.L. Wang, J. Sun, R. Zhang, X.Y. Sun, Int J Pharm, 388 (2010) 223-230.
[180] V. Bugatti, G. Gorrasi, F. Montanari, M. Nocchetti, L. Tammaro, V. Vittoria, Appl Clay Sci, 52 (2011) 34-40.
[181] V. Anand, R. Kandarapu, S. Garg, Drug Discov Today, 6 (2001) 905-914.
[182] P. Cai, Q. Huang, X. Zhang, H. Chen, Soil Biol Biochem, 38 (2006) 471-476.
[183] K. Saeki, M. Sakai, Microbes Environ, 24 (2009) 175-179.
[184] M.G. Lorenz, W. Wackernagel, Appl Environ Microb, 53 (1987) 2948-2952.
[185] E. Paget, L.J. Monrozier, P. Simonet, Fems Microbiol Lett, 97 (1992) 31-39.
[186] W.H. Yu, N. Li, D.S. Tong, C.H. Zhou, C.X. Lin, C.Y. Xu, Appl Clay Sci, 80-81 (2013) 443-452.
[187] C. Aguzzi, P. Cerezo, C. Viseras, C. Caramella, Appl Clay Sci, 36 (2007) 22-36.
[188] A.J.A. Aquino, D. Tunega, G. Haberhauer, M.H. Gerzabek, H. Lischka, J Phys Chem A, 106 (2002) 1862-1871.
[189] S. Demaneche, L. Jocteur-Monrozier, H. Quiquampoix, P. Simonet, Appl Environ Microb, 67 (2001) 293-299.
[190] F. Poly, C. Chenu, P. Simonet, J. Rouiller, L.J. Monrozier, Langmuir, 16 (2000) 1233-1238.
[191] M. Franchi, E. Bramanti, L.M. Bonzi, P.L. Orioli, C. Vettori, E. Gallori, Origins Life Evol B, 29 (1999) 297-315.
[192] P. Cai, J. Zhu, Q.Y. Huang, L.C. Fang, W. Liang, W.L. Chen, Colloid Surface B, 69 (2009) 26-30.
[193] G.W. Beall, D.S. Sowersby, R.D. Roberts, M.H. Robson, L.K. Lewis, Biomacromolecules, 10 (2009) 105-112.
[194] F.H. Lin, C.H. Chen, W.T.K. Cheng, T.F. Kuo, Biomaterials, 27 (2006) 3333-3338.
[195] J.B. Swadling, P.V. Coveney, H.C. Greenwell, J Am Chem Soc, 132 (2010) 13750-13764.
[196] K. Kalantar-zadeh, J.Z. Ou, T. Daeneke, A. Mitchell, T. Sasaki, M.S. Fuhrer, Appl Mater Today, 5 (2016) 73-89.
[197] M. Bibes, J.E. Villegas, A. Barthelemy, Adv Phys, 60 (2011) 5-84.
[198] H.H. Fan, Z.L. Zhao, G.B. Yan, X.B. Zhang, C. Yang, H.M. Meng, Z. Chen, H. Liu, W.H. Tan, Angew Chem Int Edit, 54 (2015) 4801-4805.
[199] Y. Chen, D.L. Ye, M.Y. Wu, H.R. Chen, L.L. Zhang, J.L. Shi, L.Z. Wang, Adv Mater, 26 (2014) 7019-+.

[200] Y.W. Hao, L. Wang, B.X. Zhang, D. Li, D.H. Meng, J.J. Shi, H.L. Zhang, Z.Z. Zhang, Y. Zhang, International journal of nanomedicine, 11 (2016) 1759-1778.
[201] R. Kurapati, K. Kostarelos, M. Prato, A. Bianco, Adv Mater, 28 (2016) 6052-6074.
[202] H.U. Lee, S.Y. Park, S.C. Lee, S. Choi, S. Seo, H. Kim, J. Won, K. Choi, K.S. Kang, H.G. Park, H.S. Kim, H.R. An, K.H. Jeong, Y.C. Lee, J. Lee, Small, 12 (2016) 214-219.
[203] X. Zhang, H.M. Xie, Z.D. Liu, C.L. Tan, Z.M. Luo, H. Li, J.D. Lin, L.Q. Sun, W. Chen, Z.C. Xu, L.H. Xie, W. Huang, H. Zhang, Angew Chem Int Edit, 54 (2015) 3653-3657.
[204] X. Ling, H. Wang, S.X. Huang, F.N. Xia, M.S. Dresselhaus, Proceedings of the National Academy of Sciences of the United States of America, 112 (2015) 4523-4530.
[205] H. Wang, X.Z. Yang, W. Shao, S.C. Chen, J.F. Xie, X.D. Zhang, J. Wang, Y. Xie, J Am Chem Soc, 137 (2015) 11376-11382.
[206] Z.B. Sun, H.H. Xie, S.Y. Tang, X.F. Yu, Z.N. Guo, J.D. Shao, H. Zhang, H. Huang, H.Y. Wang, P.K. Chu, Angew Chem Int Edit, 54 (2015) 11526-11530.
[207] P. Yasaei, B. Kumar, T. Foroozan, C.H. Wang, M. Asadi, D. Tuschel, J.E. Indacochea, R.F. Klie, A. Salehi-Khojin, Adv Mater, 27 (2015) 1887-+.
[208] W. Zhao, Z. Xue, J. Wang, J. Jiang, X. Zhao, T. Mu, Acs Appl Mater Inter, 7 (2015) 27608-27612.
[209] J.D. Shao, H.H. Xie, H. Huang, Z.B. Li, Z.B. Sun, Y.H. Xu, Q.L. Xiao, X.F. Yu, Y.T. Zhao, H. Zhang, H.Y. Wang, P.K. Chu, Nature communications, 7 (2016).
[210] R.C. Lv, D. Yang, P.P. Yang, J.T. Xu, F. He, S.L. Gai, C.X. Li, Y.L. Dai, G.X. Yang, J. Lin, Chemistry of Materials, 28 (2016) 4724-4734.
[211] W. Chen, J. Ouyang, H. Liu, M. Chen, K. Zeng, J. Sheng, Z. Liu, Y. Han, L. Wang, J. Li, L. Deng, Y.N. Liu, S. Guo, Adv Mater, 29 (2017).
[212] W. Tao, X.B. Zhu, X.H. Yu, X.W. Zeng, Q.L. Xiao, X.D. Zhang, X.Y. Ji, X.S. Wang, J.J. Shi, H. Zhang, L. Mei, Adv Mater, 29 (2017).
[213] C. He, K. Lu, D. Liu, W. Lin, J Am Chem Soc, 136 (2014) 5181-5184.
[214] C.Y. Sun, C. Qin, X.L. Wang, Z.M. Su, Expert Opin Drug Del, 10 (2013) 89-101.
[215] X. Zhou, F. Laroche, G.E.M. Lamers, V. Torraca, P. Voskamp, T. Lu, F. Chu, H.P. Spaink, J.P. Abrahams, Z. Liu, Nano Research, 5 (2012) 703-709.
[216] S.K. Singh, M.K. Singh, P.P. Kulkarni, V.K. Sonkar, J.J. Gracio, D. Dash, Acs Nano, 6 (2012) 2731-2740.
[217] J. Zhang, L. Feng, X. Tan, X. Shi, L. Xu, Z. Liu, R. Peng, Particle & Particle Systems Characterization, 30 (2013) 794-803.
[218] J. Joo, E.J. Kwon, J. Kang, M. Skalak, E.J. Anglin, A.P. Mann, E. Ruoslahti, S.N. Bhatia, M.J. Sailor, Nanoscale Horizons, 1 (2016) 407-414.
[219] T. Liu, C. Wang, X. Gu, H. Gong, L. Cheng, X. Shi, L. Feng, B. Sun, Z. Liu, Advanced Materials, 26 (2014) 3433-3440.
[220] L. Li, W. Gu, J. Chen, W. Chen, Z.P. Xu, Biomaterials, 35 (2014) 3331-3339.
[221] J.-H. Choy, S.-Y. Kwak, Y.-J. Jeong, J.-S. Park, Angewandte Chemie

International Edition, 39 (2000) 4041-4045.
[222] K. Ladewig, M. Niebert, Z.P. Xu, P.P. Gray, G.Q. Lu, Applied Clay Science, 48 (2010) 280-289.
[223] A. Li, L. Qin, W. Wang, R. Zhu, Y. Yu, H. Liu, S. Wang, Biomaterials, 32 (2011) 469-477.
[224] Y. Wong, K. Markham, Z.P. Xu, M. Chen, G.Q. Lu, P.F. Bartlett, H.M. Cooper, Biomaterials, 31 (2010) 8770-8779.
[225] Y. Chen, D. Ye, M. Wu, H. Chen, L. Zhang, J. Shi, L. Wang, Advanced Materials, 26 (2014) 7019-7026.